Division of Molecular Structural Biology
Department of Medical Biochemistry and Biophysics
Karolinska Institutet, Stockholm, Sweden

Structural Basis of Cysteine Biosynthesis and Peptidoglycan Remodelling in *Mycobacterium tuberculosis*

Dominic Böth

Karolinska Institutet

Stockholm 2014

Published by Karolinska Institutet. Printed by Åtta.45 Tryckeri AB

ISBN 978-91-7549-388-6

ABSTRACT

Mycobacterium tuberculosis is the causative agent of tuberculosis, which is responsible for 1.3 million deaths annually. Treatment is difficult due to an elaborate defense machinery, which includes specific metabolic changes of the bacilli upon exposure to antibiotics and the immune response of the host. The emergence of multi-drug-resistant and extremely drug-resistant strains further complicates the treatment. Therefore the development of novel antibiotics and the investigation of new unexploited targets are of high importance. In the scope of this work, potential drug targets from the L-cysteine biosynthesis and the mycobacterial cell envelope maintenance were investigated.

Cysteine biosynthesis provides promising drug targets due to a direct connection between L-cysteine availability and redox homeostasis of the bacilli. Disruption of the mycobacterial redox defense leads to attenuated growth. Three cysteine synthases are encoded in the mycobacterial genome of which CysK1 and CysM have been characterized previously. In this work CysK2 has been enzymatically characterized, catalyzing the formation of L-cysteine from O-phosphoserine and sulfide in a pyridoxal-5-phosphate-dependent reaction.

The importance of the cell wall integrity makes it a well exploited target of a broad range of antibiotics. Potent inhibitors and first-line antibiotics are currently in clinical use such as isoniazid and ethambutol, which target biosynthetic pathways of the mycobacterial cell wall. RipA, a protein of the NlpC/p60 family was previously validated as essential for infectivity. The characterized NlpC/p60 proteins are peptidoglycan hydrolases and are involved in cell division and peptidoglycan recycling. In *M. tuberculosis*, four proteins represent this family: RipA, RipB, RipC and RipD. Here we report the biochemical and biophysical characterization of RipA, RipB and RipD as well as their high resolution structures. The detailed understanding of these enzymes prepares the ground for structure-based inhibitor development targeting this enzyme family. RipA and RipB hydrolyze the peptidoglycan peptide stem between D-glutamyl- and meso-diaminopimelic acid residues. RipD is the first NlpC/p60 protein, which adapted to a non-catalytic peptidoglycan-binding function and most likely acts as a scaffold or regulatory protein.

The integrity and stability of the peptidoglycan layer is vital for intracellular survival of *M. tuberculosis*. L,D- and D,D-transpeptidases strengthen the peptidoglycan layer to withstand chemical and physical stress by the formation of 3-3 and 3-4 cross-links, respectively. The genome of *M. tuberculosis* encodes five orthologues, the L,D-transpeptidases Ldt_{Mt1-5}. The three-dimensional structure of Ldt_{Mt2} consists of three domains: two smaller domains of the Ig-fold-type segments of the protein (A and B domain) and the transpeptidase domain (C domain). The structure of the two fragments AB domain and BC domain, which are comprising the entire periplasmic part of the enzyme, gives insights to the arrangement of the peptidoglycan layers in the mycobacterial cell wall. Additionally, Ldt_{Mt2} has been identified as an off-target for β-lactam antibiotics by the formation of acyl-enzyme complexes with penam and penem class β-lactams.

LIST OF PUBLICATIONS

I. Eva Maria Steiner, **Dominic Böth**, Robert Schnell and Gunter Schneider. CysK2 (Rv0848): The Third Cysteine Synthase in *Mycobacterium tuberculosis*. *Manuscript.*

II. **Dominic Böth**, Gunter Schneider and Robert Schnell. Peptidoglycan remodeling in *Mycobacterium tuberculosis*: Comparison of structures and catalytic activities of RipA and RipB. *Journal of Molecular Biology. (2011). 413, 247–260.*

III. **Dominic Böth**, Eva Maria Steiner, Atsushi Izumi, Gunter Schneider and Robert Schnell RipD (Rv1566c) from *Mycobacterium tuberculosis*: adaptation of an NlpC/p60 domain to a non-catalytic peptidoglycan-binding function. *Biochemical Journal. (2013). 457, 33–41.*

IV. **Dominic Böth**, Eva Maria Steiner, Daniela Stadler, Ylva Lindqvist, Robert Schnell and Gunter Schneider. Structure of LdtMt2, an L,D-transpeptidase from *Mycobacterium tuberculosis*. *Acta Crystallographica Section D Biological Crystallography. (2013). D69, 432–441.*

TABLE OF CONTENTS

LIST OF ABBREVIATIONS

AM	D-arabino-D-mannan
APS	Adenosine-5'-phosphosulfate
EMB	Ethambutol
GlcNAc	N-acetyl-α-D-glucosamine
GSH	Glutathione
HMW	high molecular weight
iE-Dap	γ-D-glutamyl-meso-diaminopimelic acid
INH	Isonicotinylhydrazine (Isoniazid)
iNOS	inducible nitric oxide synthase
LAM	Lipoarabinomannan
LM	Lipomannan
LTBI	latent tuberculosis infection
LXA4	Lipoxin A4
Manp	α-D-mannopyranosyl
MDR-TB	Multi-drug-resistance tuberculosis disease
MPI	Mannosyl phosphate inositol
MSH	Mycothiol
Mur	Muramic acid
MurNAc	N-acetyl-α-D-muramic acid
NTPs	national TB control programs
OAS	O-acetylserine
OPS	O-phospho-L-serine
PAPS	3'-phosphoadenosine-5'-phosphosulfate
PAS	p-aminosalicylic acid
PBP	Penicillin-binding protein
PDB	protein data bank
PG	Peptidoglycan
PGE2	Prostaglandin E2
PIMs	Phospho-myo-inositol mannosides
PLP	Pyridoxal-5-phosphate
PZA	Pyrazinamide
RIF	Rifampicin
RNI	reactive nitrogen intermediate
ROI	reactive oxygen intermediate
TAG	Triacyl glycerol
TB	Tuberculosis disease
tri-Dap	L-alanyl-γ-D-glutamyl-meso-diaminopimelic acid
Trx	Thioredoxin

1. *MYCOBACTERIUM TUBERCULOSIS*

During the last two decades, tuberculosis (TB) has been recognized as a major global health problem since it is one of the leading causes of death among infectious diseases worldwide. The WHO estimated the total number of new infections with 8.7 million and recorded 1.3 million reported deaths of which about 300.000 have been HIV-associated TB deaths in 2012. In 1993, the WHO implemented a five component package as a strategy to contain TB comprising political commitment, proper diagnostics, supply of first line antibiotics, pursuit of communication and social mobilization to facilitate the report within the national TB control programs (NTPs) and program-based operation research. Geographically, the highest incidence rates are reported and estimated in Africa and Asia (Figure 1). About 40% of all TB cases can be located to China and India; however, the highest rates of cases and deaths per capita are in sub-Saharan Africa. About 0.5 million cases and 74.000 deaths are extrapolated in the group of children younger than age of 15. In 2011, 5.8 million newly diagnosed cases were reported to the NTPs. After administration of first line medication, a treatment success in 85% of the patients has been documented globally[1]. Worldwide, about 20% of TB-positive patients are estimated to be infected with multi-drug-resistant TB (MDR-TB).

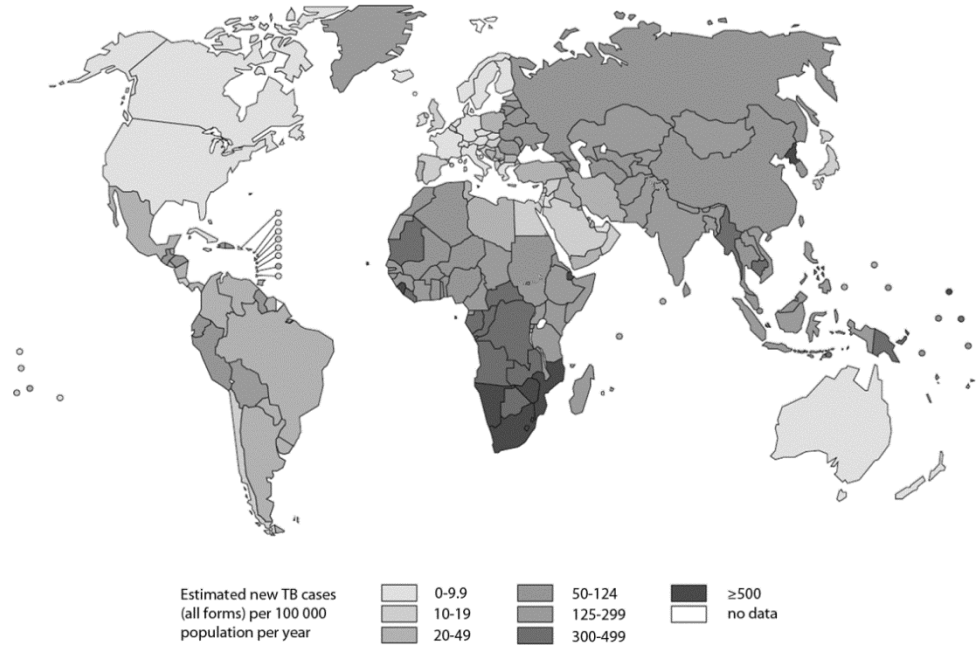

Figure 1: Map indicating the estimated number of new TB cases worldwide according to the Global Tuberculosis Report 2013[1]

1.1 ACTIVE AND LATENT FORM OF THE TUBERCULOSIS DISEASE

Mycobacterium tuberculosis has been first discovered by Robert Koch as the causative agent of TB, which typically affects the lungs, but also other organs. The expulsion of bacteria from TB-positive patients spread the disease; however only a smaller number of patients infected with *M. tuberculosis* is developing active TB.

Primary TB is pulmonary, but the bacilli can disseminate within the host when left untreated. The common way of transmission of mycobacteria is airborne, to date the exact dose for a spread resulting in disease development is unclear[2,3]. Active TB is usually characterized by an initial lung inflammation followed by the phagocytosis of the bacilli by alveolar macrophages. If no treatment is administered, the disease leads to death. Commonly, a cluster of infected macrophages start to form multi-nucleated Langerhans cells in the lung parenchyma followed by a specific immune response, which initiates the formation of granuloma coinciding with a self-destructive formation of lesions in the lung[4,5]. In terminal stages of the active infection, tissue damage aggravates and leads to expulsion of bacilli by coughing.

A *M. tuberculosis*-specific immune response in absence of a clinical manifestation of the disease defines the state of a latent TB infection (LTBI)[6]. *M. tuberculosis* enters lung tissue and persists in primary phagosomes of alveolar macrophages by arresting phagosome maturation[7]. During LTBI, the immune system of the host is able to contain the bacilli by rendering them in a non-replicative state, but the host is unable to clear the infection. The formation of productive granulomas follows, which is common in LTBI. They are originating from interaction of naïve T cells with infected macrophages[8,9]. Antigens from *M. tuberculosis* are processed by antigen-presenting cells, which in turn lead to a specific immune response, but not to a complete clearance.

Recommended standard for the reliable diagnosis of TB are the sputum microscopy and the culture in liquid medium. Commonly, drug susceptibility tests are conducted in parallel. As a more cost-effective method, solid culture media are suggested and frequently used in resource poor countries[10]. PCR screening, imaging and immunohistochemical examination of biopsy samples support the diagnosis of active TB[11]. An estimate of 30% of TB-positive patients and about 90% of MDR-TB-positive patients remain undiagnosed in low income countries[1].

1.2 FIRST LINE DEFENSE – MACROPHAGES AND NEUTROPHILS

It could be experimentally shown that the fort mechanism of immune response following an infection of the airways is the diapedesis of phagocytic cells including alveolar macrophages, dendritic cells and neutrophils. The phagocytes engulf the bacilli and contribute to the first line of defense by the expression of antimicrobial peptides (Figure 2)[12–16]. The phagocytes orchestrate the action of the other components of the immune system via cytokine production. Macrophage and neutrophil response is therefore critical for the outcome of the immune response to mycobacteria, which could either promote bacterial clearance or containment, the latter resulting in the development of LTBI[17,18].

M. tuberculosis mediates macrophage signaling via scavenger receptors, complement receptors and mannose receptors, leading to the formation of the phagosome[19]. In the case of nonviable mycobacteria, phagolysosomal fusion occurs (e.g. upon IFN-γ signaling) and the bacilli are lysed. On the contrary, viable and virulent *M. tuberculosis* prevents the phagosome from maturation: a fusion of the phagosomal and the lysosomal compartment is impeded and bacterial clearance fails[8,13]. Dissemination of bacteria thereafter results in the activation of a T cell response in the lung-draining mediastinal lymph nodes (Figure 3).

M. tuberculosis can induce necrotic cell death within the macrophages, which allows the bacilli to be released from the cell and spread (Figure 2). A very potent alternative protective mechanism of the macrophage is the single cell apoptosis as well as contact-dependent apoptosis leading to the delivery of the compartmentalized bacilli along with the apoptotic debris to the lysosome in which the bacteria are killed; a process called efferocytosis[20,21]. Efferocytosis further supports the process of sequestration of compartmentalized bacteria and subsequent clearance[22] (Figure 2). Mycobacteria however display virulence mechanisms which inhibit the induction of apoptosis[23,24]. SecA2 has been identified as a key player in the inhibition of apoptosis. The gene encodes for a component of a virulence-associated protein secretion system. Deletion of secA2 results in enhanced apoptosis and increased priming of antigen-specific $CD8^+$ and $CD4^+$ T ells[24].

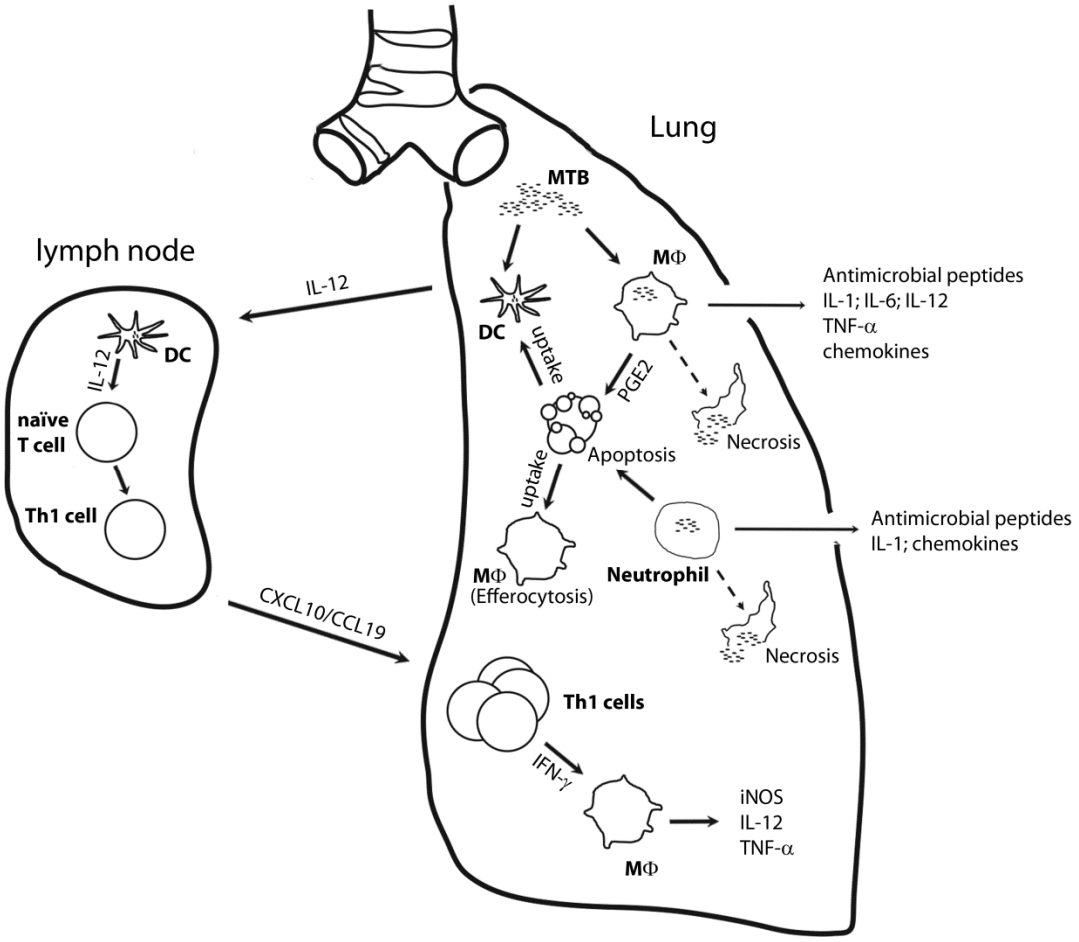

Figure 2: Schematic representation of the cellular defense mechanisms of the host within the lung tissue. *M. tuberculosis* is engulfed by dendritic cells (DCs), macrophages (MΦ) and neutrophils. DCs activate naïve T cells upon IL-12 signaling, which do enter the site of infection thereafter to induce inflammation. The fate of MΦ is dependent on the signaling of PEG2, which promotes apoptosis, which in turn leads to efferocytosis and a subsequent killing of bacilli. MΦ necrosis leads to the dissemination of the bacilli. Neutrophils can also undergo apoptosis and necrosis, the exact signaling however remains elusive. Infected MΦ and neutrophils activate the synthesis of antimicrobial peptides as well as various cytokines.

The type of cell death of macrophages, apoptosis or necrosis, is regulated by eicosanoids, prostaglandin E2 (PGE2) and lipoxin A4 (LXA4). By induction of LXA4 and repression of PGE2, mycobacteria evoke necrosis and apoptosis is avoided, resulting in cell-to-cell spread of bacteria (Figure 2). Alveolar macrophages of $Alox5^{-/-}$ mice infected with *M. tuberculosis* display the tendency to undergo apoptosis[25,26]. In parallel to the antimicrobial action of macrophages, neutrophils fulfill a detrimental role in pathogenesis of TB. They facilitate activation of naïve antigen-specific $CD4^+$ T cells during the course of infection and promote the adaptive immune system by direct interaction with DCs, which in turn are more effective activators of $CD4^+$ T cells. Neutrophils activate immune signaling via IL-6 and IL-17; the IFN-γ signaling however remains unaffected[27].

1.3 FORMATION OF GRANULOMAS AS A RESULT OF HUMAN IMMUNE RESPONSE

The exact role of granuloma formation during an infection with *M. tuberculosis* is not known. It is suggested that granulomas participate in the protection of the host against an uncontrolled spread of bacilli, on the other hand their contribution to tissue pathology is discussed and even the promotion of infection has been imputed[27]. However, the different stages of the granuloma seem to depend on the progression of disease and immune response. Innate and adaptive immunity control the morphology of granulomas[8,9,28].

The tubercular granulomas contain infected macrophages in their center, which have differentiated into multi-nucleated giant cells, epithelioid cells, foamy macrophages harboring lipid droplets and neutrophils[29]. This core is surrounded by lymphocytes ($CD4^+$ and $CD8^+$ T cells and B cells) and fibroblasts, which produce the peripheral fibrotic capsule. Proinflammatory and inhibitory cytokines play a key role in the formation of granulomas[27,30].

The presence of the necrotic core appears as a secondary result to cell lysis and creates a hypoxic hostile environment. The same types of granulomas have also been found in infected guinea pigs and nonhuman primates used as model organisms, but not in mice[31]. In LTBI, bacilli reside within the central hypoxic environment where they undergo drastic metabolic changes. In the situation of an active infection, replication of the bacilli occurs mainly in the oxygenated areas[28]. It has been proposed that mycobacteria create a supportive environment within the granuloma e.g. through manipulation of the macrophage lipid metabolism[29].

1.4 ANTIBIOTIC TREATMENT AND DRUG RESISTANCE

Despite evolutionary pressure, aggravation of drug-resistant TB is to a large extent the result of interrupted or inadequate TB therapy. It threatens global efforts to control the global TB epidemic and is a major concern of public health in several countries. MDR-TB is defined by resistance against two of the most commonly administered antibiotics, isoniazid (INH) and rifampicin (RIF). According to the WHO, the rates of new MDR-TB cases are highest in Eastern Europe and Russia. About 20% of the new cases are diagnosed as MDR-TB. The total number of MDR-TB cases however is estimated for India and China, which account for almost 40% of all MDR-TB cases worldwide.

Extensively drug-resistant TB (XDR-TB) displays resistance against all members of the fluoroquinolones and at least one of the three injectable second line drugs in addition to INH and RIF[1,32,33].

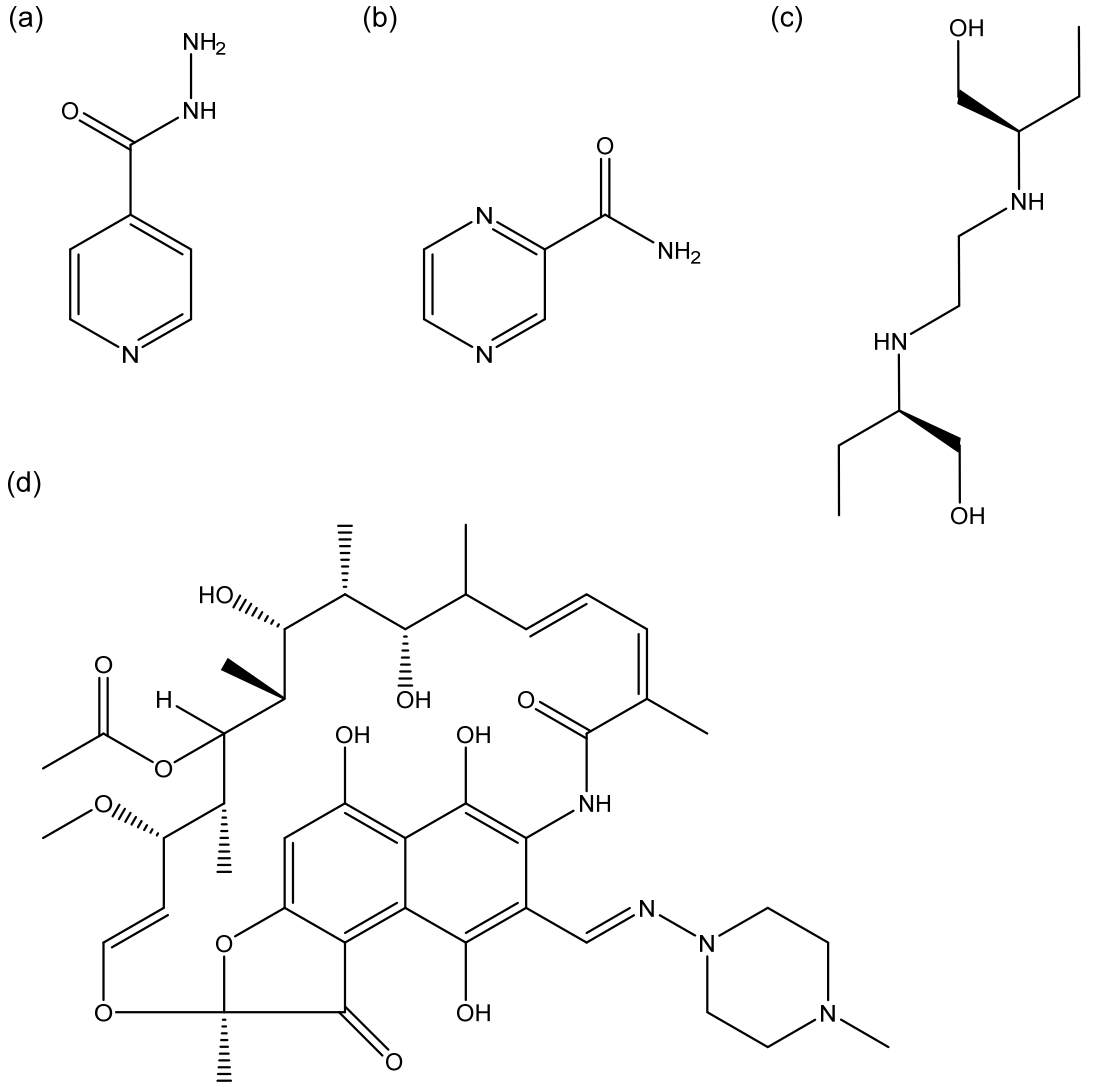

Figure 3: First-line antibiotics used for short course treatments. (a) Isonicotinylhydrazine (Isoniazid, INH), (b) Pyrazinamide (PZA), (c) Ethambutol (EMB), (d) Rifampicin (RIF)

In general, drug-resistance occurs due to chromosomal mutations in a low proportion of *M. tuberculosis* in pan-sensitive strains. Combined drug treatment is meant to prevent the emergence of drug-resistant bacteria. The first positive effect of combined drug administration has been seen in combination therapy of *M. tuberculosis* with streptomycin and p-aminosalicylic acid (PAS). Emergence of streptomycin-resistance could be largely prevented in presence of PAS[34,35]. After the introduction of INH, PAS

has quickly been replaced, followed by regimens of INH and streptomycin. In 1960, after emergence of drug-resistance against INH, PAS or streptomycin, a triple therapy for at least 12 months with all three became standard treatment in Europe. Almost half of the patients failed to complete the treatment[36]. Modern short course treatments were possible after the development of RIF and PZA. This regimen gives four drugs: INH, RIF, PZA and EMB[37,38] (Figure 3). The simultaneous use of several drugs in combination contained drug-resistance remarkably. Non-continuous drug administration, treatment interruptions as well as changes in treatment based on side effects, pharmacokinetic interactions and inconstancy in compliance result in mechanisms, which allow the emergence of drug resistance[39]. Recently, also totally drug-resistant TB has been described[1,40,41]. To meet this problem, new effective drugs and the identification of potent drug targets are required[42].

In view of this alarming situation, much of the current research about *M. tuberculosis* is focused on host-pathogen interaction including the complex immune answer upon mycobacterial infection as well as the development of vaccines and potent novel drugs to contain the bacilli from an epidemic spread. The identification of new target proteins or essential genes, which in turn can be targeted with potent antibiotics exhibiting new mechanisms of action, is of high relevance. Structure-based drug discovery, phenotypic screening and detailed biochemical understanding will aid on this route.

2. OXIDATIVE STRESS – SMALL MOLECULES AS POTENT ROI/RNI SCAVENGERS

During infection and transmission, *M. tuberculosis* encounters oxidative stress. During LTBI, bacilli are residing in granulomas of alveolar macrophages, where they are confronted with hypoxic stress and nutritional deprivation[31,43].

2.1 REDOX HOMEOSTASIS

Maintenance of a redox balance is crucial for every organism; catabolic and anabolic processes need to effectively be separated from each other. Elaborate machineries counteracting redox stress imposed by macrophages are necessary to maintain redox homeostasis. Five well characterized redox couples play a key role: $NADH/NAD^+$, $NADPH/NADP^+$, mycothiol, thioredoxins and peroxiredoxins. Under normoxic conditions, the $NADH/NAD^+$ ratio is favoring high levels of NAD^+ for efficient electron extraction through catabolic reactions[44]. Under hypoxic conditions however, the ratio changes by an accumulation of NADH, suggesting reductive stress during pathogenesis[44], which also leads to resistance against INH[45]. Inhibition of reoxidation of $NADH/FADH_2$ results in a disruption of redox homeostasis and inhibits bacterial growth.

One can distinguish two sources of oxidative stress *M. tuberculosis* encounters: endogenous and exogenous stress. Endogenous stress is characterized by endoxidation of carbon chains using O_2 as the final electron acceptor involving one-electron transfer in the respiratory chain as well as stress induced by bactericidal drugs. Exogenous stress is generated by the immune response of the host. Macrophages and neutrophils are producing ROI and RNI. The formation of a superoxide radical ($O_2^{-}\cdot$) can serve as a precursor of RNI[46,47]. The generation of $O_2^{-}\cdot$ is catalyzed by a single electron reduction of O_2 by the NADPH oxidase e.g. in macrophages and neutrophils. H_2O_2 is produced by a reaction of two $O_2^{-}\cdot$ catalyzed by superoxide dismutase, which in turn can react to highly reactive hydroxyl radicals ($HO\cdot$) through a Fenton reaction[48]. It has been suggested that a number of bactericidal antibiotics act along the formation of $HO\cdot$[49], this however has been questioned recently by experimental data excluding a correlation of antibiotic treatment and ROI production[5051].

ROI and RNI have been shown to potently kill several pathogenic species, including various mycobacterial strains, where H_2O_2 and $O_2^{-\cdot}$ are the most abundant ROI. However, the exact role of ROI in *M. tuberculosis* remains elusive[52–54]. On the other hand, the role of RNI in TB is more defined by effectively killing *M. tuberculosis in vitro*[55]. Murine macrophages and epithelial alveolar lung cells express iNOS and produce significant levels of nitric oxide (NO) capable of killing mycobacteria[56–58]. Interestingly, NO is also a signal for the bacterium to enter dormancy, by inhibiting respiration and growth[59].

M. tuberculosis exhibits a sophisticated mechanism of sensing redox stress. In place of classical sensors like FNR, OxyR or SoxR, which are absent in the mycobacterial genome, it encodes for DosRST. The DosRST genes have been shown to be approximately 50-fold up-regulated in hypoxic conditions[60–62]. Besides oxygen depletion, the regulon is also activated by NO and carbon monoxide (CO) inside host lesions[59,63,64]. DosR has been characterized further as the transcriptional master regulator for dormancy and is controlled by the two histidine kinases DosS and DosT, which in turn are detectors of the impairment of respiration[62,65,66]. The transcription factor WhiB has been identified as a potent redox sensor. WhiB harbors an $O_2^{-\cdot}$- and NO-responsive iron/sulfur cluster and is a major player in coordinating the metabolic response of *M. tuberculosis* upon changes in redox homeostasis[67,68].

2.2 SUSTAINING THE THIOL-REDOX STATUS IN *M. TUBERCULOSIS*

Thiol compounds are providing the redox control in all living organisms. A balanced thiol pool is also vital for *M. tuberculosis* to survive within the host. The reductive milieu of the cytosol of the bacilli is maintained by multiple thiol buffers, which can occur in millimolar concentration[69]. The primary reducing systems are based on mycothiol (MSH), a disaccharide, which is equivalent to glutathione (GSH), and the thioredoxin (Trx) system.

2.2.1 MSH

In nature, GSH is the most abundant low-molecular-weight thiol compound (Figure 4). Most actinobacteria however deploy MSH instead of GSH. MSH consists of glucosamine, myo-inositol and N-acetylcysteine and is the major low molecular weight thiol compound in *M. tuberculosis* (Figure 4). MSH biosynthesis is therefore dependent

of L-cysteine synthesis[70]. Under ROI and RNI stress, MSH is necessary to maintain survival of *M. tuberculosis*[71,72]. MSH funnels the reaction cycle by reducing a reaction partner under formation of a mixed disulfide. Oxidized MSH is thereafter reduced by mycothiol reductase in a NADPH-dependent reaction. Only recently, mycoredoxins catalyzing the reduction of oxidized MSH have been found in mycobacteria and subsequently in other actinobacteria[73]. The *de novo* synthesis of MSH requires 5 steps: The initial reaction is the formation of the glycoside bond between N-acetylglucopyranosyl-inositol phosphate, which is subsequently dephosphorylated and deacetylated, followed by the condensation of L-cysteine and the subsequent acetylation of the L-cysteine to form active MSH[74] (Figure 4). The MSH biosynthetic pathway has been recognized as a promising drug target, since it is unique for actinobacteria and essential for growth and survival of *M. tuberculosis*[71,72]. First inhibitors have been developed following a structure-based approach against the enzyme MshC, which catalyzes the condensation of L-cysteine to the disaccharide[75,76]. In *M. tuberculosis,* MSH is present at millimolar concentrations. Interestingly, bacilli void of MSH after knock-out of MshC upregulate the biosynthesis of the thiourea derivative ergothioneine, which is involved in the redox balance[77,78].

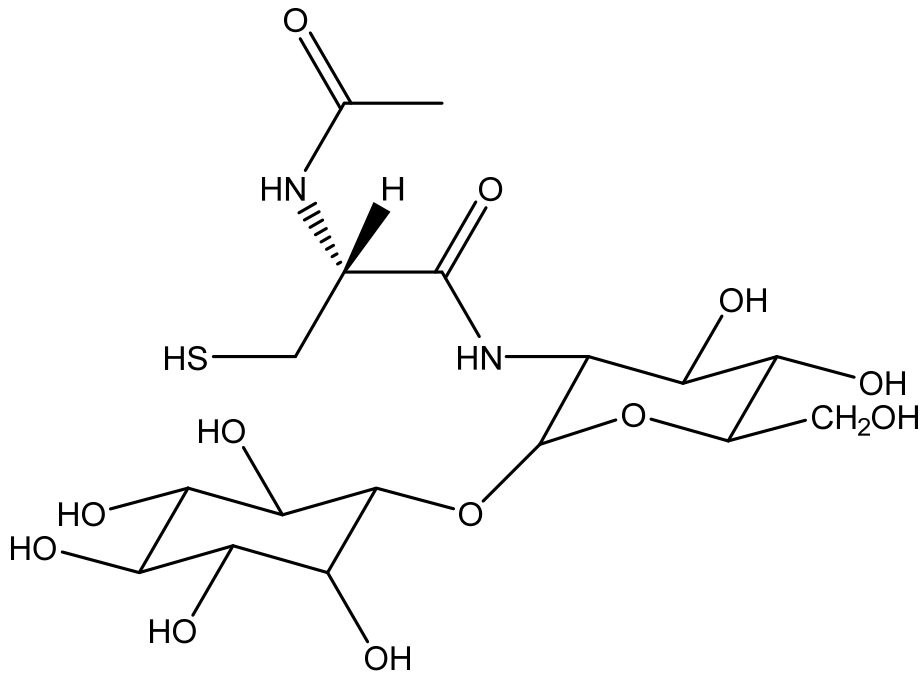

Figure 4: Mycothiol as a potent radical scavenger in *M. tuberculosis*. It consists of a disaccharide condensed to an acetylated L-cysteine residue. The thiol group of the cysteine represents a reduced sulfur species important for redox homeostasis.

2.2.2 Thioredoxin

Thioredoxins (Trxs) have been characterized as systemic disulfide reductases sustaining a reductive environment. Trxs cycle between a reduced and an oxidized state and show a conserved WCXXC motif[79,80]. Oxidized Trxs are reduced by thioredoxin reductase (TrxR) in a FAD- and NADPH-dependent reaction[81]. *M. tuberculosis* codes for TrxA, TrxB and TrxC[82], which have been shown to be non-essential[83], indicating the redundancy of the system. In contrast, TrxR is essential and distinct from the mammalian enzyme and could therefore be an important drug target[84]. Peroxiredoxins (Prxs) have been linked to the electron transfer from Trxs[85,86] and function as scavengers for hydroperoxides and peroxynitrites.

2.3 SULFUR METABOLISM IN *M. TUBERCULOSIS*

Bacteria of the Actinomycetales group produce mycothiol, a L-cysteine containing disaccharide as a potent radical scavenger for maintenance of redox homeostasis[70]. This links the availability of cysteine and therefore reduced sulfur species directly to the redox defense of *M. tuberculosis*. As a response to redox stress during LTBI, genes involved in sulfur and cysteine metabolism have been shown to be upregulated[87–89], which could be validated by a mutagenesis screen based on transposon insertions into genes related to cysteine metabolism leading to phenotypes more susceptible to defense mechanisms of the host cell[83,90].

The biosynthesis of sulfur-containing compounds is tightly connected to the sulfur assimilation pathway[91], which is a pathway catalyzing the uptake and the metabolism of sulfate from the host[92]. Sulfate ,which enters the bacterial cell via an active transport is subsequently adenylated by the ATP sulfurylase CysD (Rv1285) / CysN (Rv1286), resulting in the formation of adenosine 5'-phosphosulfate (APS), which can either be directly reduced leading to sulfite (SO_3^{2-}) and AMP by the APS reductase CysH (Rv2391)[93] or phosphorylated by the APS kinase (Rv1286; C-terminal domain) to form 3'-phosphoadenosine-5'-phosphosulfate (PAPS). PAPS is an abundant sulfate donor of sulfotransferases that produce metabolites like sulfolipid-1[94]. The sulfite derived from the reductive branch of the APS/PAPS pathway is further reduced by SirA (NirA, Rv2391) to hydrogen sulfide (H_2S) representing the sulfur source for reduced sulfur metabolites. Key enzymes involved in the cysteine biosynthetic pathways are SirA, a ferredoxin-dependent sulfite reductase, CysK1 (OASS-A; Rv2334)[95], a pyridoxal-5-

phosphate (PLP)-dependent O-acetylserine (OAS) sulfhydrylase[96], CysM (Rv1336)[97] and CysK2 (Rv0848), both O-phospho-L-serine (OPS)-dependent cysteine synthases (Figure 5), CysE (Rv2335), which catalyzes the formation of OAS, substrate for CysK1 from serine in a CoA-SH-dependent reaction[98] and CysO as sulfur donor for the CysM-catalyzed reaction[97,99] (Figure 5).

2.3.1 SirA (Rv2391)

SirA catalyzes a six-electron reduction of sulfite to sulfide (S^{2-}) providing the reduced sulfur for sulfur-containing amino acids[95]. Thus, SirA allocates the necessary sulfide derived from the sulfur assimilation pathway for the OAS-dependent cysteine *de novo* synthesis. The enzyme was annotated as a ferredoxin-dependent sulfite/nitrite reductase; both substrates are accepted by the enzyme depending on the metabolic state of *M. tuberculosis*. Enzymes of this family contain a combination of a [Fe_4-S_4] iron/sulfur cluster and a siroheme and exhibit ~20% sequence identity to NADPH-dependent sulfite reductases, e.g. found in *E. coli* and are usually monomeric, while the *E. coli* homologue forms an oligomeric complex[95].

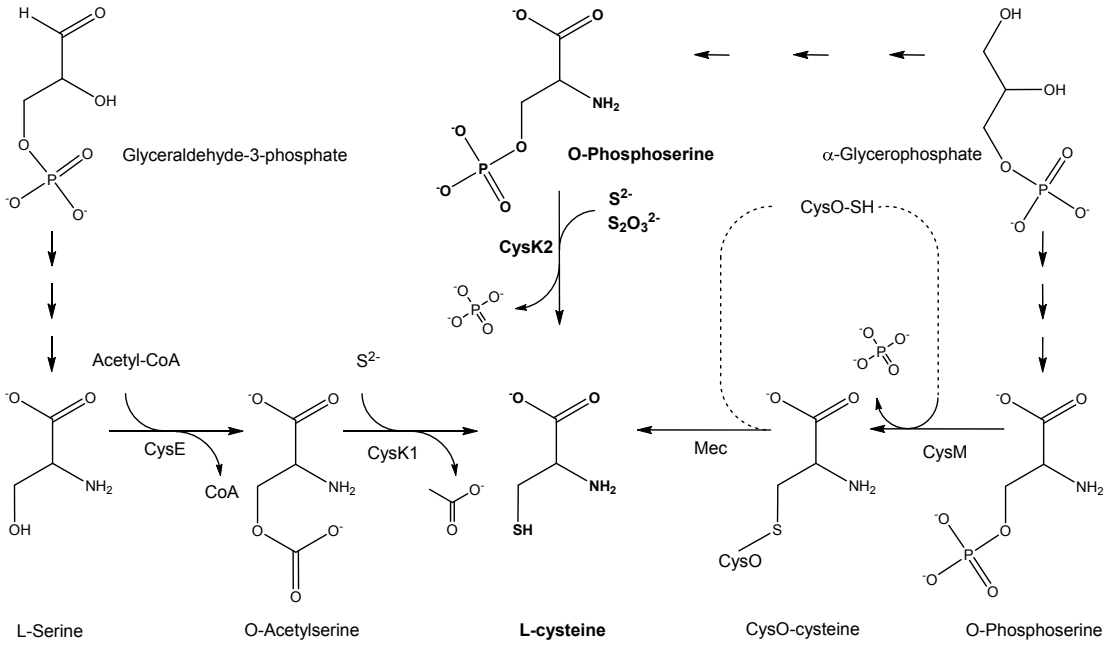

Figure 5: The biosynthetic pathways for the *de novo* cysteine synthesis in *M. tuberculosis*. The canonical pathway is dependent on CysE and CysK1, which catalyze the synthesis of cysteine from serine via OAS and sulfide. The alternative pathway is catalyzed by CysM. This pathway requires the availability of OPS as acceptor substrate and thiocarboxylated CysO-SH as sulfur donor. The third pathway is based on CysK2, characterized in this work. The substrate preference reflects a combination of CysK1 and CysM. CysK2 utilizes OPS as acceptor and sulfide as donor substrate.

2.3.2 Three cysteine synthases in the mycobacterial genome

Three genes in the genome of *M. tuberculosis* are annotated to encode for the cysteine synthases CysK1 (Rv2334), CysM (Rv1336) and CysK2 (Rv0848). CysK1 shares ~37% sequence identity with CysM and ~26% with CysK2. CysM and CysK2 have about 27% identity (Figure 6). The overall fold of CysK1 and CysM is similar to type II family of PLP-dependent enzymes. However, functional studies revealed distinct differences in substrate specificity. The acceptor substrate of CysK1 is OAS, which reacts with sulfide as a sulfur source[96]. CysM is dependent on OPS and thiocarboxylated CysO as sulfur donor[97,100]. CysK2 is characterized by a utilization of OPS and sulfide as shown in this work (paper I). In this sense CysK2 is a combination of CysK1 and CysM regarding substrate specificity.

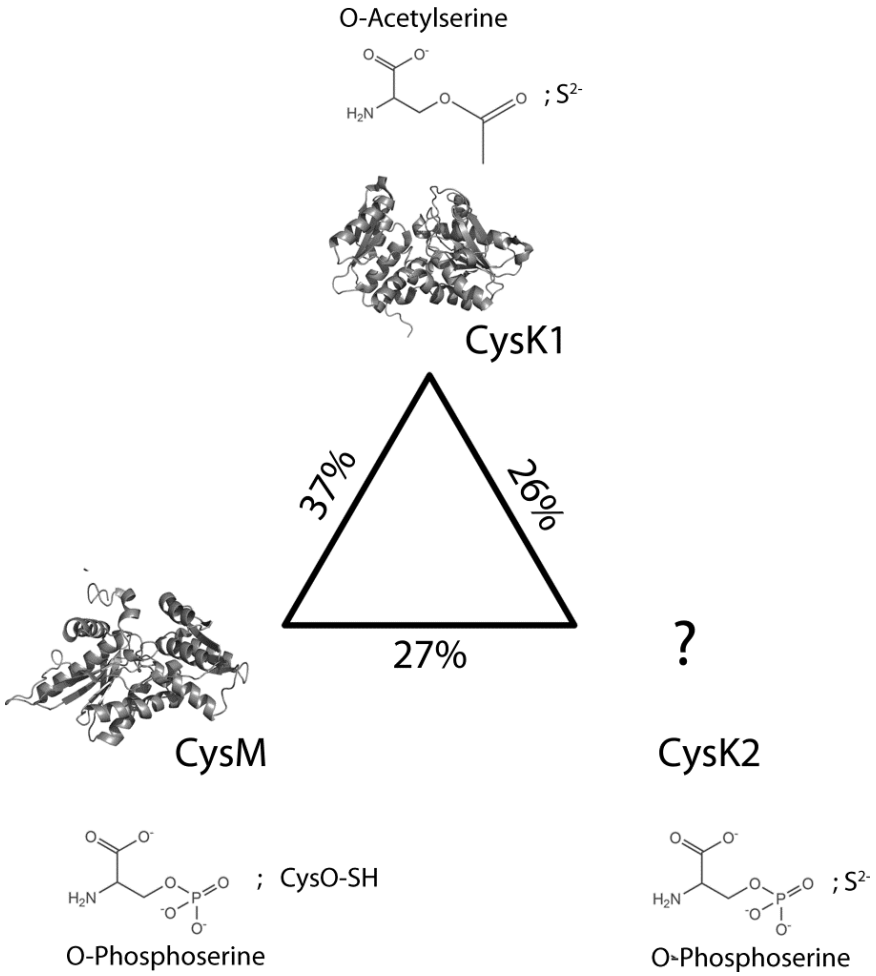

Figure 6: L-Cysteine synthases in *M. tuberculosis*. Respective substrates are indicated as well as sequence identity between the three enzymes.

2.3.3 CysK1 (Rv2334) – the classical pathway for L-cysteine

De novo synthesis of cysteine in plants, archaea and many eubacteria starts with the acetylation of serine, catalyzed by an L-serine acetyl transferase (CysE; Rv2333). The product O-acetylserine is then further converted to L-cysteine in a PLP-dependent reaction. This step involves the elimination of acetate and the addition of H_2S obtained during the reductive branch of the sulfur assimilation pathway by the enzyme O-acetylserine sulfhydrylase, denoted as CysK1 (Rv2334) in *M. tuberculosis*[96].

The crystal structure of CysK1 has been solved and used to elucidate the structural basis of catalysis by this enzyme[96]. Similar to other PLP-dependent reactions, the mechanism of CysK1 follows a reaction mechanism divided into two half reactions. Once OAS enters the active site of the enzyme, the formation of the external aldimine releases the invariant lysine residue, which formed the internal aldimine in the ground state of the enzyme (Figure 7).

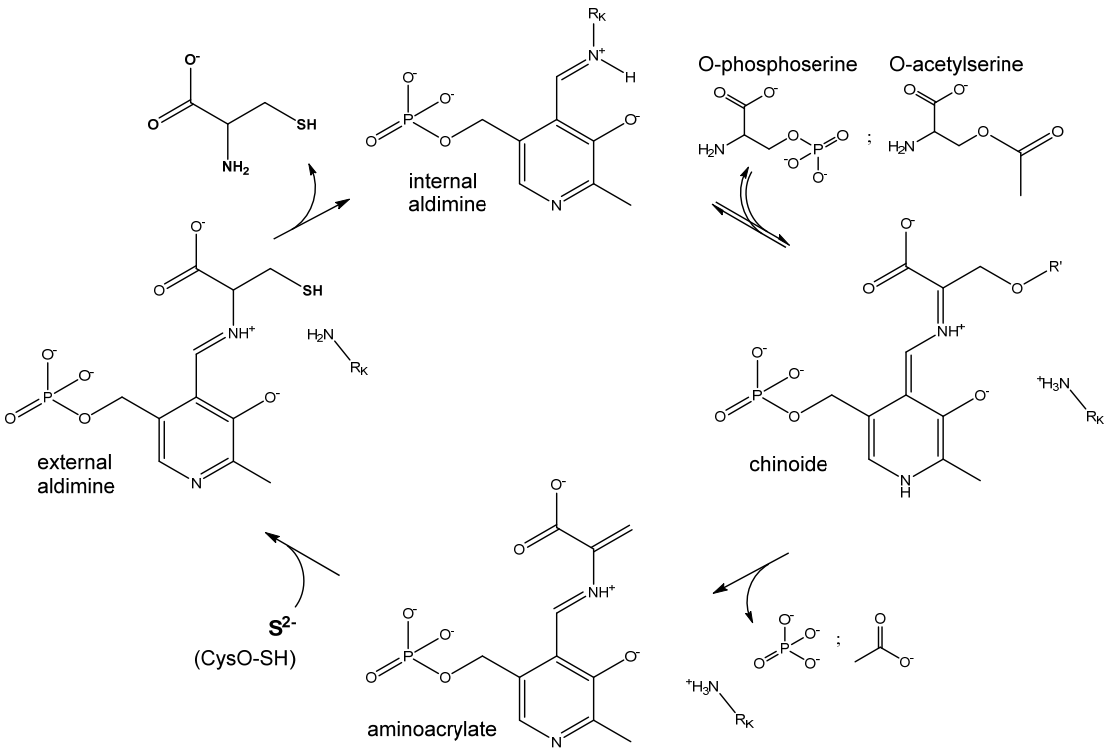

Figure 7: Summarized catalytic mechanisms of CysK1, CysM and CysK2. The α-amino group of the acceptor substrate OPS/OAS displaces the ε-amino group of the active site lysine residue resulting in the formation of an external aldimine. Elimination of the OAS acetate or OPS β-phosphate leads to the formation of the aminoacrylate intermediate. Nucleophilic attack at the Cβ of this intermediate by sulfide or CysO-SH results in the formation of L-cysteine or L-cyteinyl-CysO, which is released, returning the enzyme to the ground state.

After formation of the external aldimine, a proton is abstracted by an acid-base reaction catalyzed by the active site lysine, which acts as base and the acetate group of OAS is eliminated to conclude the first half reaction with the formation of the aminoacrylate intermediate (Figure 7). The second half reaction is initiated by the nucleophilic anti-addition of the incoming sulfide at the β-carbon and results in an L-cysteine-PLP external aldimine. Upon reprotonation of the C-α-atom by the invariant lysine, L-cysteine is released and the internal aldimine is restored (Figure 7). The correct stereo-specificity is ensured by the specific orientation of the aminoacrylate in the active site pocket, the mode of reprotonation by the invariant lysine residue and a rearrangement of the enzyme allowing the nucleophile to react[96].

The catalytic activity of CysK1 is competitively inhibited by the regulatory nature of a C-terminal tetrapeptide stretch (DFSI) of CysE suggesting the formation of a bi-enzyme complex[101]. This regulatory function of the tetrapeptide stretch of CysM has also been observed for the bi-enzyme complex of homologues in *H. influenza* and *A. thaliana*[102–104]. Co-crystallization of CysK1 with the tetrapeptide revealed the binding mode of this inhibitory ligand. DFSI binds at the active site cleft between the two domains of CysK1 and extends to the enzyme surface.

On basis of the CysK1-DFSI complex, high-throughput virtual screening and energy-based pharmacophore modeling has been conducted leading to the identification of more potent inhibitors[105,106]. The binding mode of one of the strong hits was elucidated by X-ray crystallography. Based on the 2.0 Å structure of this enzyme-ligand complex, improved inhibitors in the low nM range have been developed.

2.3.4 CysM (Rv1336) – an alternative cysteine synthase

CysM has been identified as a phospho-L-serine sulfhydrylase in *M. tuberculosis* utilizing thiocarboxylated CysO as a sulfur donor for the subsequent *de novo* biosynthesis of L-cysteine, which clearly separates this pathway from the OAS-dependent one (Figure 5)[97,107].

The reaction cycle of CysM, as a type II family of PLP-containing enzyme, is similar to that of CysK1[108]. The resting state of the enzyme forms an internal aldimine between the invariant lysine and PLP. Binding of OPS leads to the formation of the external aldimine, which eventually eliminates the β-phosphate from OPS resulting in the same aminoacrylate intermediate common in type II PLP enzymes. Burns et al. showed in functional studies that CysM uses a novel mode of sulfur delivery[109]. CysO, a small

thiocarboxylated protein, binds and reacts with the aminoacrylate intermediate leading to the formation of a covalent cysteinyl-CysO adduct in an external aldimine with the PLP (Figure 7). Re-protonation of the α-carbon releases the cysteinyl-CysO from the enzyme and the internal aldimine-ground state is restored. Cysteinyl-CysO is then hydrolyzed by a zinc-dependent metalloprotease (Rv1334)[109].

It is noteworthy that the oxidation-sensitive aminoacrylate intermediate in CysM is not prone to unspecific nucleophilic attack[97]. Active site closure protects the reaction intermediate from unspecific side reactions by maintaining a closed conformation of the active site providing a safe cysteine synthesis under conditions of oxidative stress, relevant during LTBI. The C-terminal pentapeptide of CysM (GQLWA) is instrumental for this conformational change, which also contributes to sulfur donor selectivity towards CysO[100].

Biochemical characterization of CysM and CysO revealed an alternative pathway for the *de novo* biosynthesis of L-cysteine, which by the dependence of OPS and thiocarboxylated CysO differs from the OAS-dependent L-cysteine synthesis.

2.3.5 CysK2 (Rv0848) – *paper I*

Besides the two previously described cysteine synthases the genome of *M. tuberculosis* encodes *cysk2* (Rv0848), a third gene related to OASS sulfhydrylases, which is induced under oxidative stress and hypoxia[59], suggesting a link of its expression to LTBI. On the protein sequence level, CysK2 shares about 28% sequence identity with mycobacterial CysK1 and CysM, respectively.

We cloned, expressed, purified and characterized CysK2 as the third L-cysteine synthase in the mycobacterial genome (paper I). CysK2 uses OPS as acceptor substrate and sulfide as sulfur donor in a PLP-dependent reaction. The reaction mechanism of CysK2 resembles that of a type II family PLP-dependent enzyme and can therefore be subdivided into two half-reactions. The first half-reaction concludes in the formation of the aminoacrylate reaction intermediate after formation of the external aldimine with the acceptor substrate OPS (Figure 7). Thereafter L-cysteine is produced by the elimination of the phosphate group of OPS and the reaction of sulfide with the aminoacrylate. Subsequently, the internal aldimine with the invariant Lys65 is restored, returning the enzyme to the ground state.

Solution studies of recombinant CysK2 by circular dichroism (CD) spectroscopy revealed a mixed α/β secondary structure, which compares well to that of the two

homologues in *M. tuberculosis*, CysK1 and CysM. The sequence identity between CysK2, CysK1 and CysM is ~28%. Distinctive motifs of PLP-dependent enzymes are highly conserved between the three homologues including the invariant Lys65 in CysK2 and the sequence stretch ^{201}GTGGT^{205}, which is coordinating the co-factor. Smaller alterations in the amino acid sequence coordinating the carboxyl group of the incoming substrate are manifest in CysK2 (^{90}ESTGGTLG^{97}) compared to CysK1 and CysM. Interestingly, CysK2 shows also differences at the N-terminal and C-terminal ends, which are missing in the two homologues (Figure 9). The characteristic absorption spectrum typical for class II family PLP enzymes could be observed, confirming the presence of PLP in CysK2 (Figure 10).

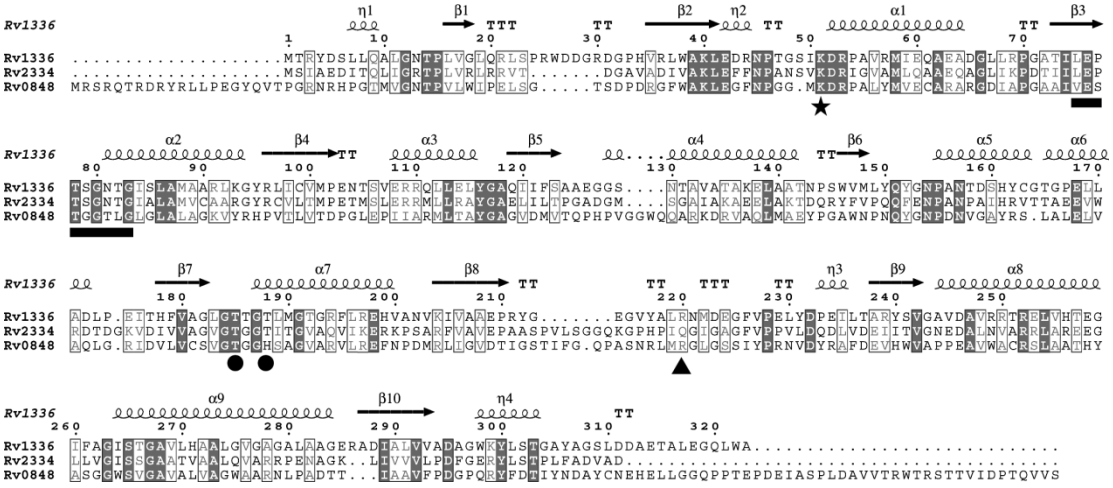

Figure 8: Structure-based multiple sequence alignment of three homologue cysteine synthases in *M. tuberculosis*.

After testing various putative substrates, a similar reaction to that of CysM revealed OPS as acceptor substrate for CysK2, which has been confirmed spectrophotometrically by a significant shift of the absorbance from 412 nm resembling the internal aldimine state[110] to 465-470 nm characteristic for the aminoacrylate intermediate. These changes during the reaction cycle are common for PLP-dependent enzymes[96,97,111] (Figure 9). Unlike in the case of CysM, the aminoacrylate intermediate is not very stable, indicating a different role of the C-terminal extension compared to the stabilizing role of the C-terminal residues of CysM[100].

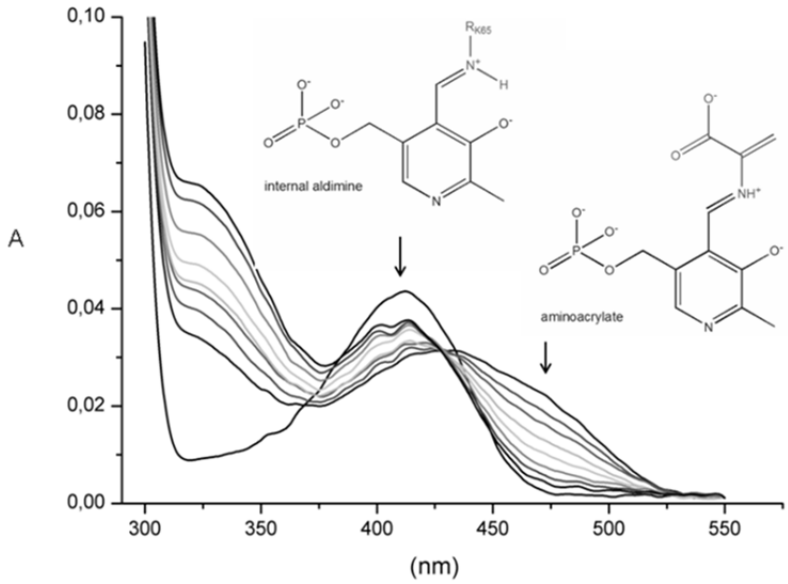

Figure 9: UV/Vis spectra of CysK2. The UV/Vis spectrum of CysK2 shows the specific internal aldimine related maximum at 412 nm (black line). Addition of 2 mM OPS results in fast enzyme-aminoacrylate intermediate formation. Spontaneous decay of the aminoacrylate intermediate is demonstrated by the set of spectra recorded after 3, 6, 9, 14, 20, 30, 40 and 55 minutes following addition of the substrate (gray).

The fast formation of the aminoacrylate could be assessed by stopped-flow spectrophotometry by monitoring the specific absorbance maximum at 475 nm and the second-order rate constant was determined to be ~ $2.5 \cdot 10^3$ $M^{-1}s^{-1}$ that compares well with CysM. The phosphate release upon formation of the aminoacrylate could be measured in a malachite-green-based assay and revealed that CysK2 dephosphorylates OPS in a multiple turnover with a K_M(OPS) of 233 µM and a V_{max}(OPS) of 1.3 U mg^{-1} at 22°C, where 1 U is defined as 1 µmol min^{-1}. The abundance of hydroxyl ions in the reaction buffer leads to unspecific hydrolysis of the aminoacrylate in absence of a sulfur donor. This explains a higher turnover rate at higher pH[111].

This unspecific hydrolysis of the aminoacrylate has been investigated by stopped flow photometry and compared to the reaction in presence of the sulfur source. The presence of 2 mM sulfide increased the consumption of the aminoacrylate 60-times. The reaction product L-cysteine has been verified by the acid-ninhydrin assay[112], which allows the specific spectrophotometric detection of L-cysteine. Kinetic parameters have been determined for the sulfide driven reaction resulting in a $V_{max}(Na_2S)$ of 0.5 U mg^{-1}; $K_M(Na_2S)$ of 374 µM and a V_{max}(OPS) of 1.0 U mg^{-1} and K_M(OPS) of 135 µM, the latter compare well with those obtained from the malachite green assay.

Arg243 in CysK2 corresponds to Arg220 of CysM (Figure 8), which was shown to be responsible for OPS specificity in CysM[97]. We have shown that Arg243 is important for OPS specificity for the reaction cycle in CysK2. Kinetic analysis of the CysK2(R243A) mutant revealed a decreased pseudo first-order rate constant in the OPS specific first half-reaction and a residual activity of 12% measured by determination of the released phosphate by the malachite green assay and about 17% in the acid-ninhydrin assay for cysteine production.

In conclusion, we have characterized CysK2 as a third PLP-dependent L-cysteine synthase in *M. tuberculosis*. The reaction cycle is dependent on OPS as acceptor substrate and sulfide as sulfur source, which is derived from the sulfur assimilation pathway. The substrate specificity is distinct from the two isoenzymes CysK1 and CysM and positions CysK2 in between the well-established routes for cysteine *de novo* synthesis. This could play a role in LTBI during which the availability of the invariant substrates due to redox stress is limited. OPS as acceptor substrate of CysK2 requires the availability of 3-phosphoglycerate, which can be allocated during hypoxia and oxidative stress within the alveolar macrophage by lipolysis and the subsequent release of glycerol, which can be phosphorylated by the glycerol kinase. These findings shed some light on the function of this enzyme, which so far has been elusive[92].

2.3.6 Targeting the cysteine biosynthesis of *M. tuberculosis*

Mutants of *M. tuberculosis* depleted in CysM that are residing in alveolar macrophages are only attenuated in growth[90] (Figure 5), hence the inhibition of only one cysteine biosynthetic pathways will probably not be sufficient to clear an infection. A complete inhibition of the L-cysteine *de novo* synthesis could rather be achieved by inhibiting three independent enzymes CysK1, CysM and CysK2 in *M. tuberculosis* during different stages of infection.

3. THE MYCOBACTERIAL CELL ENVELOPE

The mycobacterial cell envelope displays a unique architecture, which distinguishes it from those of other bacterial genera. It consists of a plasma membrane, the cell wall core, the outer membrane and capsular polysaccharides (Figure 10). The cell wall core is built by peptidoglycan (PG), which is covalently attached to arabinogalactan by a glycosidic bond via a phosphoryl-N-acetyl glucosaminosylramnose[113]. Arabinogalactan connects via an ester bond to mycolic acids, which are one dominant component of the outer membrane. It harbors further non-covalently bound glycolipids, polysaccharides and lipoglycans, which also form the surface exposed capsule[114–117].

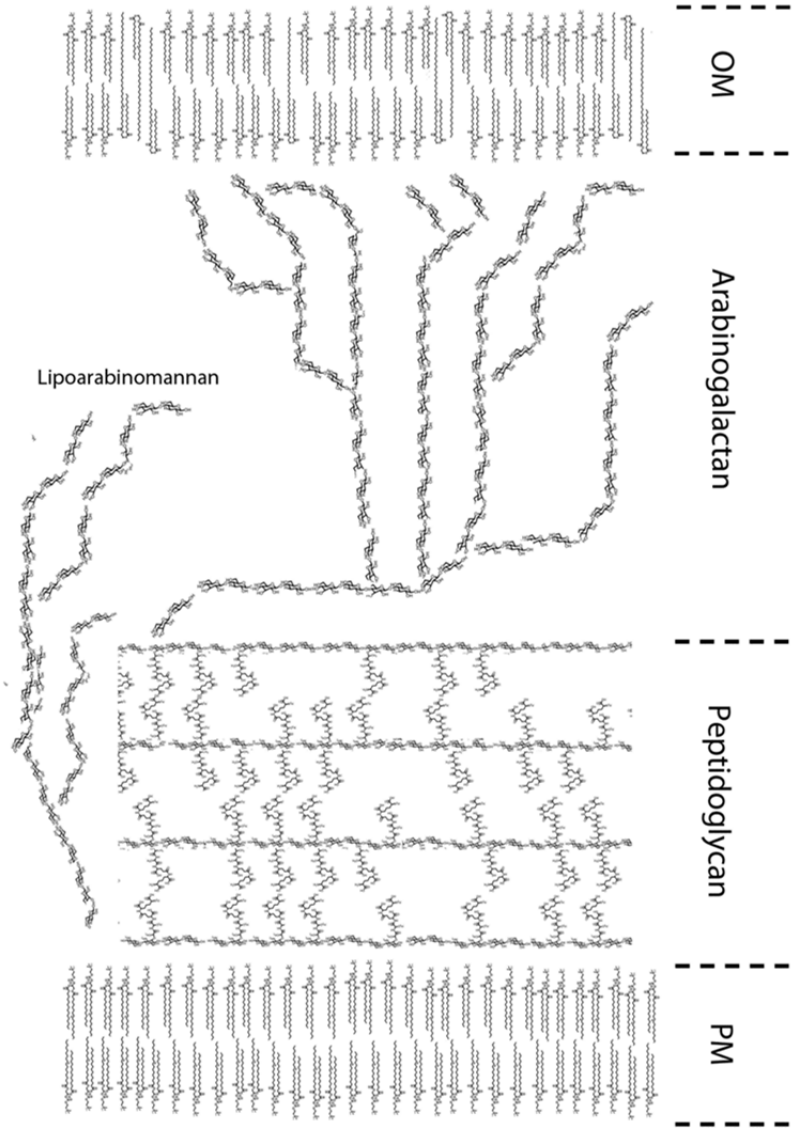

Figure 10: Schematic representation of the mycobacterial cell envelope.

3.1 THE CAPSULAR POLYSACCHARIDES

The outer surface-exposed part of the cell envelope of mycobacteria is the capsule[118], it coats bacteria and consists mainly of proteins and polysaccharides[119–121]. Three types of polysaccharides have been identified contributing to the capsular material: α-D-glucans of high molecular weight (>100 kDa) built of a core of α-1,4-glycosidic D-glucose polymers branching in oligoglucosides of D-arabino-D-mannan (AM) or D-mannan nature[122]. All sugars are devoid of charged modification such as acetylation and sulfonation. The structure of the AM is identical to that of the lipoarabinomannan (LAM), however deployed of the phosphatidyl-myo-inositol core. α-D-glucans constitute the major component of the capsule[123].

3.2 PIMS, LIPOMANNAN AND LIPOARABINOMANNAN

Mycobacteria possess amphipathic lipoglycans, LAM, lipomannan (LM) and phospho-myo-inositol mannosides (PIMs). They all share a phosphatidylinositol (PI) anchor with mannosylation extension at the 6- and 2-OH of the *myo*-inositol. PIMs are glycolipids composed of fatty acids esterified to a glycerol, which form a phosphodiester with a *myo*-inositol[124,125] (Figure 11). This phospho-myo-inositol is further substituted at C6 and C2-OH with α-D-mannopyranosyl (Manp) moieties to form PIM_2, the mannosyl phosphate inositol (MPI) anchor.

The lipid composition of the anchor is heterogeneous, with respect to number, location and nature of fatty acids. Four sites can be acylated at 1-OH and 2-OH of the glycerol unit, the 3-OH of the *myo*-inositol and the 6-OH of the mannose[126,127]. In *M. tuberculosis*, palmitic and tuberculostearic acids are the most abundant acylations. To a lesser extend myristic and ricinoleic acids are occurring[125] (Figure 11). Intermediates of differently acylated PIMs accumulate in the membrane for the synthesis of higher-order PIMs.

LM and LAM share both the same mannan core[128], which is covalently linked to PIMs. The mannan backbone is composed of α-1,6-glycosidically bound Manp residues and flanked by α-1,2-glycosidically bound Manp (Figure 11). The core is extended by the condensation of a arabinan domain consisting of linear α-1,5-glycosidic arabinofuranose (Araf) residues, which branches in a α-3,5-glycosidic manner to form two types of sugar decoration: first, linear tetra-arabinose and secondly branched hexa-arabinose motifs[129], both of which are capped by Manp in *M. tuberculosis* and *M.*

bovis[130]. PIMs, LM and LAM play a key role in arresting lysosomal fusion and endosomal fusion with the phagosome[131].

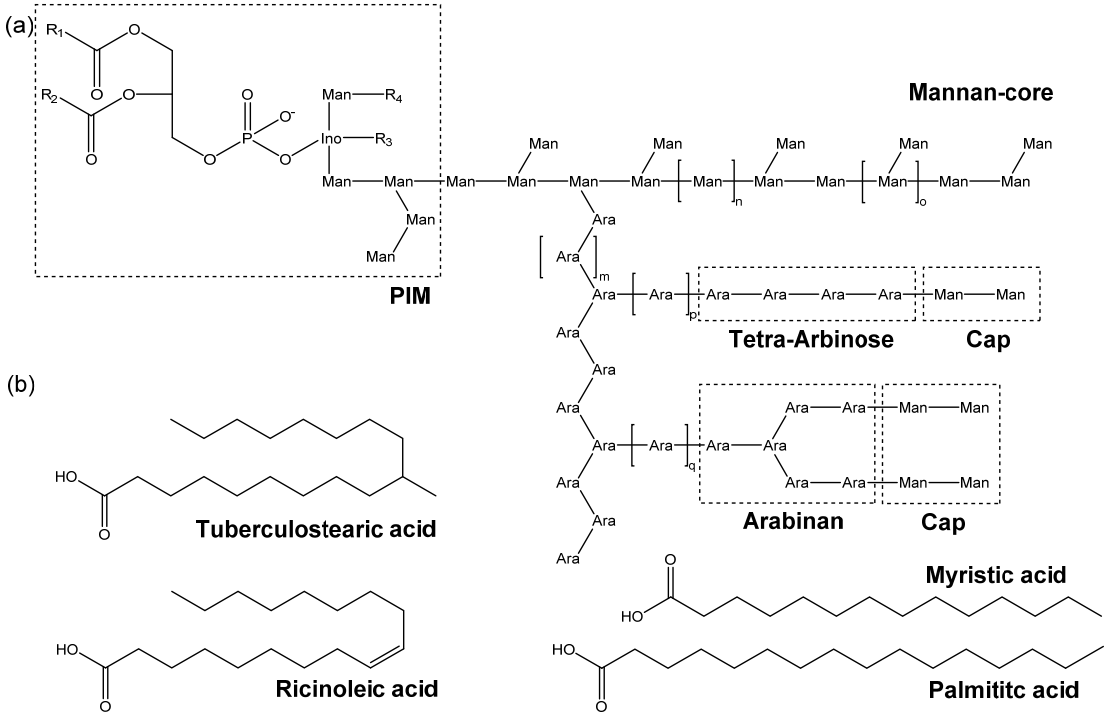

Figure 11: Cell wall components based on phospho-myo-inositol mannosides (PIMs) (a) schematic representation of the polysaccharides linked to the PIM to form various lipoglycans of the cell wall (b) fatty acids ($R_{1\text{-}4}$), which anchor the PIM in plasma membrane.

3.3 ARABINOGALACTAN

Arabinogalactan is exclusively built of furanose sugars and tethers the mycolic acids to the PG layer. The galactan domain is composed of 30 Galactofuranose (Galf) residues in β-1,5- and β-1,6-glycosidic bonds, three arabinan domains containing ~30 Araf residues α-1,3-, α-1,5- and β-1,2-glycosidically branching from the galactan at sugar positions 8, 10 and 12 and a spacer at the reducing end covalently linked to the PG via 5-D-Galf-1,4-L-Rhap-1,3-D-GlcNAc[129,132].

3.4 PEPTIDOGLYCAN

Peptidoglycan (PG) is a complex polymer forming the rigid layer of the cell wall, providing cell shape and protection against shere stress and osmotic pressure[117,133,134]. Together with the arabinogalactan layer it forms the cell wall core. To date, the orientation of the glycans of the PG layer is controversal. Most of the experimental data

suggest the glycan strands to be oriented in parallel to the cell surface, however, a second model proposed a perpendicular orientation of the glycan strands to the cell surface[134–136]. The PG of *M. tuberculosis* belongs to the classification A1γ similar to that of *E. coli* and *B. subtilis*[137]. It is composed of a backbone of alternating N-acetyl-α-D-glucosamine (GlcNAc) and muramic acids (Mur), which can be modified in various ways, however they are acylated by glycolic acid rather than acetylated[138–140]. Mur connects via the 6-OH to the arabinogalactan layer[129,134,141]. The linar polysaccharides formed by alternating units of Mur and GlcNAc are dispersed by peptide side chains of L-alanyl-D-isoglutaminyl-meso-diaminopimelyl-D-alanine. The peptide stems are in turn covalently linked to the Mur. Two peptide stems from adjacent saccharide backbones can be heavyly cross-linked. Up to 80% of the PG peptide stems are cross-linked in *M. tuberculosis*[142], whereas in *E. coli* only 50% of the PG peptide stems display the same feature[135]. The amino acids of the peptide stem can be further modified by amidation of the glutamyl and diaminopimelinyl residues[134]. Two different types of cross-links have been characterized, which are catalyzed by different transpeptidases: 3-4 cross-links, containing a D-alanyl-D-aminopimelinyl peptide bond formed by penicillin-binding proteins (PBPs) and 3-3-cross-links with different chirality between the L- and D-center of two adjacent diaminopimelic acids that are catalyzed by L,D-transpeptidases[143] (Figure 12).

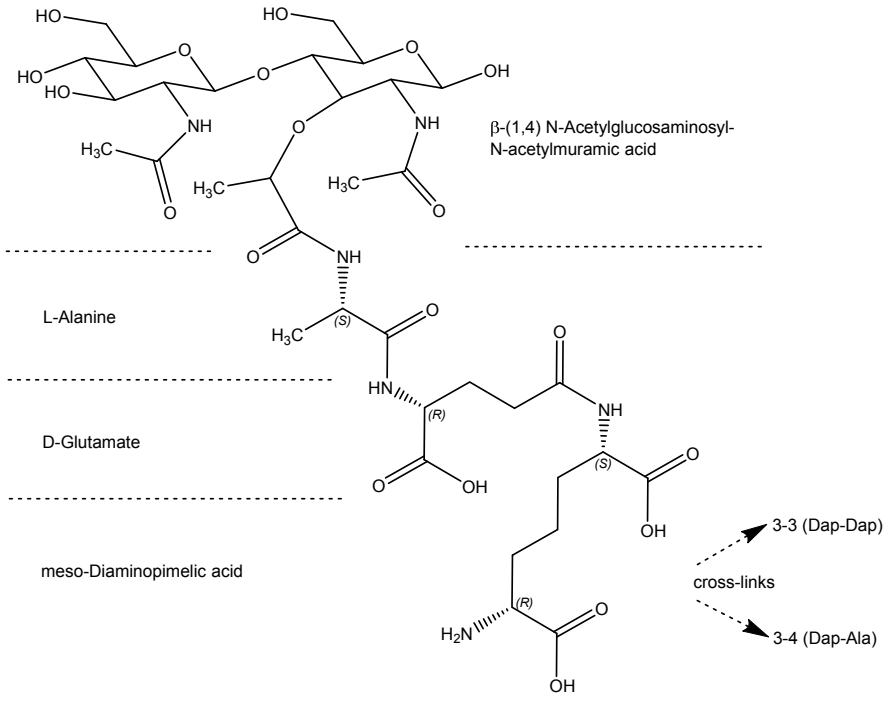

Figure 12: Chemical structure of a PG unit. MurNAc is condensed via a lactoyl linker to the tripeptide L-alanyl-D-isoglutaminyl-meso-diaminopimelic acid, which in turn is involved in cross-linking to the neigbouring peptide stem of the adjacent sugar-backbone.

3.4.1 Synthesis and remodelling of peptidoglycan

The initial step of PG synthesis is cytoplasmatic and requires the activation of N-acetylglucosamine and muramic acid to form their respective UDP-forms[144,145] (Figure 13). Thereafter the pentapeptide stem is built up on the UDP-MurNAc by sequential steps. This process is ATP-driven and involves the proteins of the Mur operon. The resulting UDP-MurNAc-pentapeptide is therafter decaprenylated (lipid I) and condensed with UDP-GlcNAc by MurG to form the membrane-anchored lipid II intermediate. Lipid II is flipped across the membrane and upon insertion in the growing glycan chain of the sacculus, the decaprenyl anchor is released[146,147] (Figure 13).

The cross-link formation within the PG sacculus subunits is catalysed by D,D-transpeptidation, forming 3-4-connections (DAP-D-Ala) and L,D-transpeptidases forming 3-3-cross-links[148] that stabilize the PG layer of the bacilli[149] (Figure 13). PBPs are globular proteins located on the exterior of the plasma membrane. They are grouped into high- and low- molecular weight PBPs. Four PBPs have been characterized as β-lactam targets in *M. tuberculosis*[150]. The *M. tuberculosis* genome encodes for five isoenzymes of L,D-transpeptidases, all of which have been identified as off-targets for β-lactam treatment[151,152].

During cell division and bacterial growth, PG remodelling requires the cleavage of covalent bonds to allow the sacculus to grow without only thickening it[144]. This follows a concerted mechanism of hydrolases of different nature including D,D- and L,D-endopeptidases (D,D-EPases, L,D-EPases), transglycosylases (RpfBs)[153], amidases[154] and NlpC/p60 proteins[155–157].

The release of PG cleavage products, also referred to as muropeptides, has been known for some time to result in the activation of immune response. NOD1 and NOD2 receptors have been shown to interact with PG fragments. Their leucine-rich repeat domain is responsible for ligand recognition. The smallest fragment recognized by NOD1 is iE-Dap, whereas NOD2-mediated signaling is activated by muramyl peptides[158].

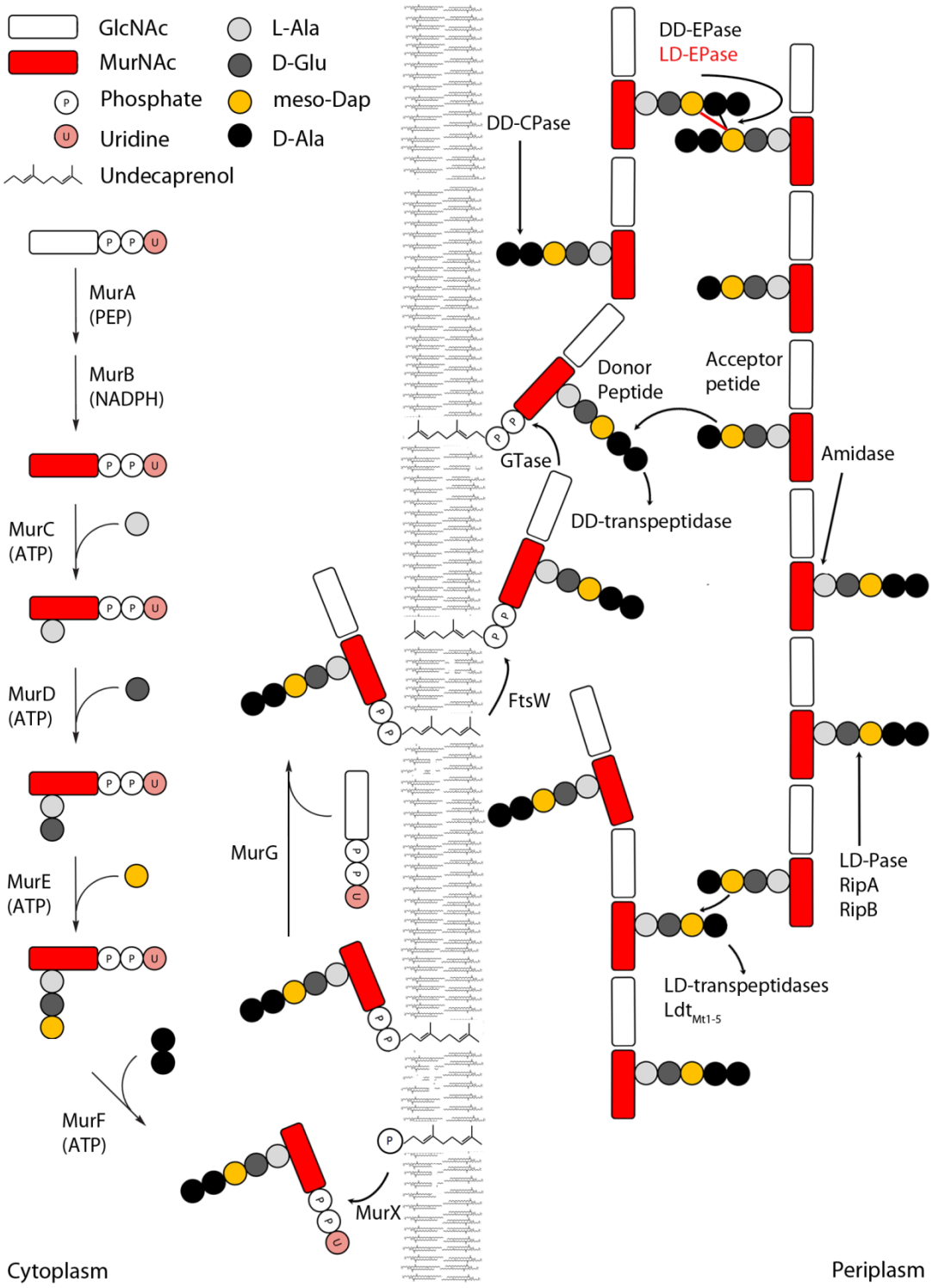

Figure 13: The synthesis and condensation of a new PG strand into the existing network. PG building blocks are synthesized in the cytoplasm, and subsequently linked to undecaprenyl phosphate and flipped across the plasma membrane. A glycosyltransferase (GTase) catalyzes the polymerization of the PG. Thereafter, the building unit is attached to the sacculus by a D,D-transpeptidase (D,D-TPase). Peptides are trimmed by D,D-, L,D-and D,L-carboxypeptidases (CPases). Cross-links are cleaved by the D,D-and L,D-endopeptidases (EPases). L,D-transpeptidases (L,D-TPases) are required for the formation of L,D-cross-links (3-3).

3.4.2 The Rip-family

In the *Mycobacterium marinum*-zebrafish model system two genes denoted as iipA (ripA) and iipB (ripB), which show partial homology, have been identified to be involved in invasion of host macrophages and intracellular persistence. Upon deletion of the iipA locus, the pathogen loses virulence and shows decreased survival within the host macrophages. Additionally, increased sensitivity to ciprofloxacin, erythromycin and the first-line drug RIF and atypical septum formation has also been observed. Interestingly, this distinct phenotype could be rescued by complementing with the *M. tuberculosis* gene Rv1477 (RipA), suggesting a similar function of the Rv1477-Rv1478-operon[155].

RipA and RipB contain a NlpC/p60 domain[156,157]. Two additional NlpC/p60 proteins are encoded in the mycobacterial genome, RipC (Rv2190c) and RipD (Rv1566c) (Figure 14 and 15). NlpC/p60 hydrolases are characterized as specific PG hydrolases involved in PG remodelling and cell division. NlpC/p60 proteins were characterized first as autolysins LytE and LytF of *L. monocytogenes* proteins p60 and p45. This family also includes the *E. coli* membrane-associated lipoprotein NlpC (termed as NlpC/p60 proteins), which possesses a conserved amino-terminal cysteine. Members of this family are characterized as endopeptidases hydrolysing the D-glutamyl meso-diaminopimelate linkage in the PG[159]. Multiple paralogues have been identified in most bacteria, which underlines their importance in PG remodelling and cell division[160].

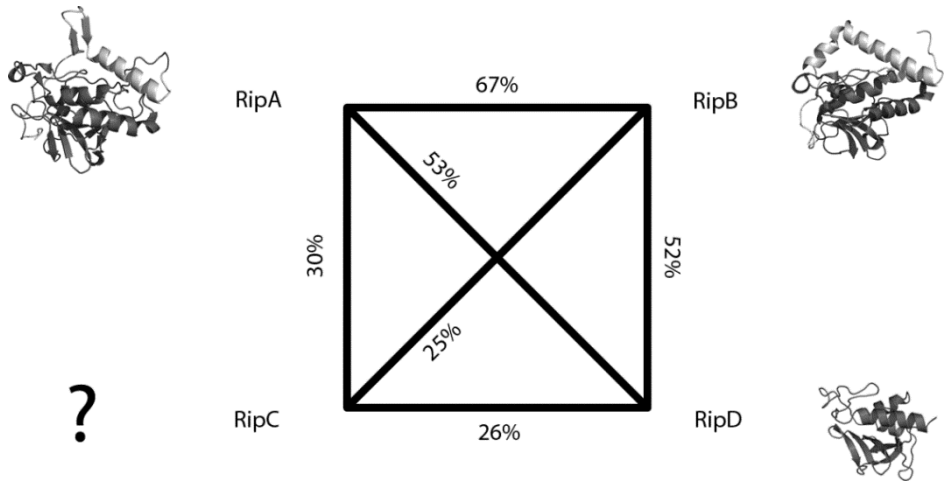

Figure 14: The four proteins of the Rip-family in *M. tuberculosis*. Sequence identities based on the NlpC/p60 core domain are indicated.

3.4.3 RipA (Rv1477) and RipB (Rv1478) – *paper II*

RipA (Rv1477) identified as a binding partner of RpfB and RpfE (resuscitation-promoting factors B and E) localizes at the septum region of dividing bacteria together with RpfB[116]. RipA and RipB proteins belong to the superfamily of NlpC/p60 hydrolases (Figure 14 and 15).

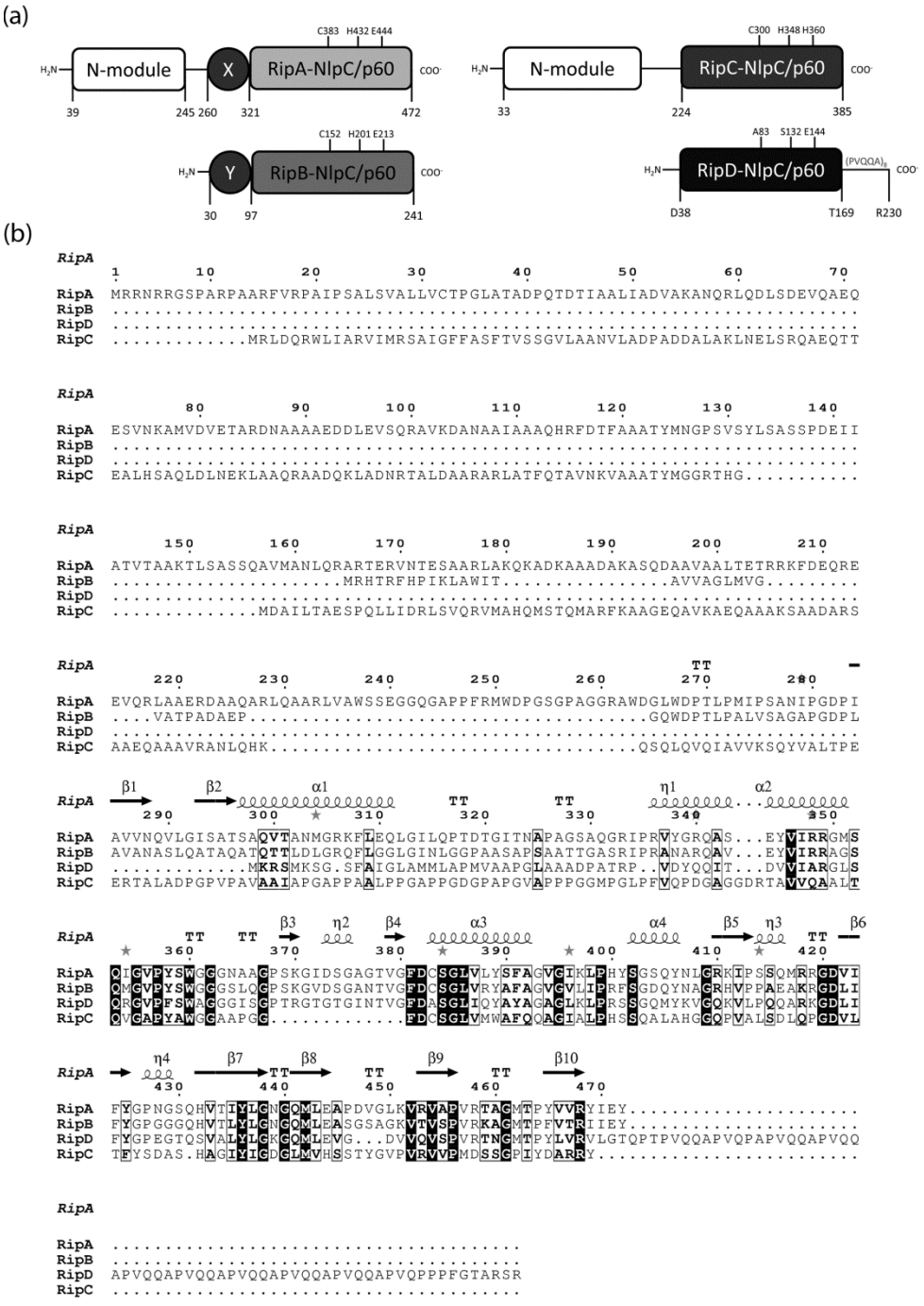

Figure 15: (a) modular organization of NlpC/p60 homologues in *M. tuberculosis*. RipA and RipC contain an additional N-terminal domain. (b) Structure-based multiple sequence alignment. RipA (PDB:3PBC) was used as a reference structure; secondary structure is indicated: β-sheet (⟶), helix (ꕥ).

Since RpfB and RpfB homologues in *M. tuberculosis* contain a lysozyme-homologue domain[161] and RipA contains a catalytically active peptidase domain, the RipA-RpfB complex can be considered as a putative PG degradation machinery combining the proposed glycosidase activity of RpfB with the peptidase activity of RipA. PBP1 (Rv0050) also interacts with the C-terminal NlpC/p60 domain of RipA, hence the formation of a PG-remodelling machinery of hydrolases, transglycosylases and transpeptidases were suggested, coordinating the cell wall remodelling[162].

RipA and RipB are encoded in the same operon and most likely expressed simultaneously. RipA is composed of two distinct domains: a so far uncharacterized N-terminal domain and the C-terminal NlpC/p60 domain. RipB is an NlpC/p60 domain protein without larger additional domains. Both proteins display a signal sequence at the N-terminus, which allows them to be transported to the periplasmic space.

Our interaction studies between RipA, RipB and their suggested substrate clearly strengthened their proposed localisation in the PG meshwork (Figure 16). Purified proteins have been tested for binding HMW-PG in a binding assay[154]. RipA and RipB accumulate in the insoluble HMW-PG.

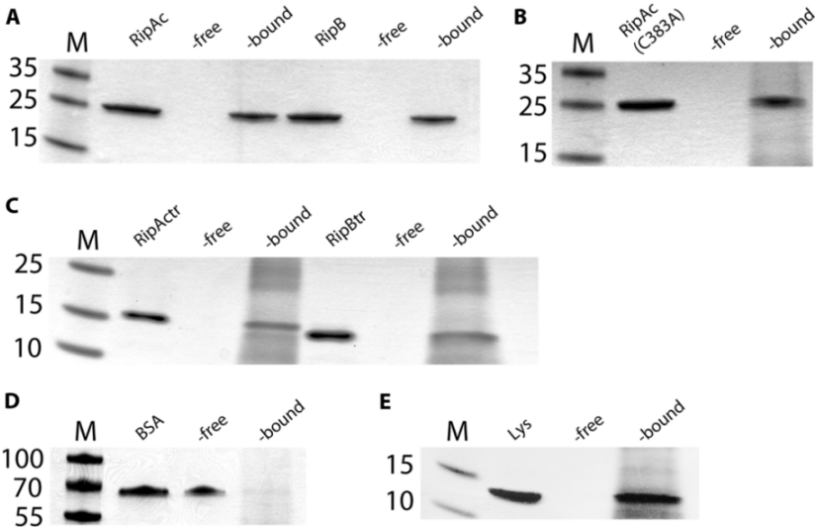

Figure 16: PG-binding experiment. (a) Fractions from the binding assay using RipAc (RipA-NlpC/p60; residues 260–472) and RipB proteins. (b) RipAc(Cys383Ala) mutant binding to HMWPG. (c) Truncated proteins RipActr and RipBtr. (d) BSA binding to HMWPG. (e) Lysozyme binding to HMWPG.

Both proteins show catalytic activity in cleaving defined soluble PG fragments e.g. γ-D-glutamyl-meso-diaminopimelic acid (iE-Dap) or L-alanyl-γ-D-glutamyl-meso-diaminopimelic acid (tri-Dap) (shown in paper II). The exact cleavage position could

be determined to be the peptide bond between iE-Dap. A more detailed proposal for the enzymatic mechanism has been described[157] (Figure 17).

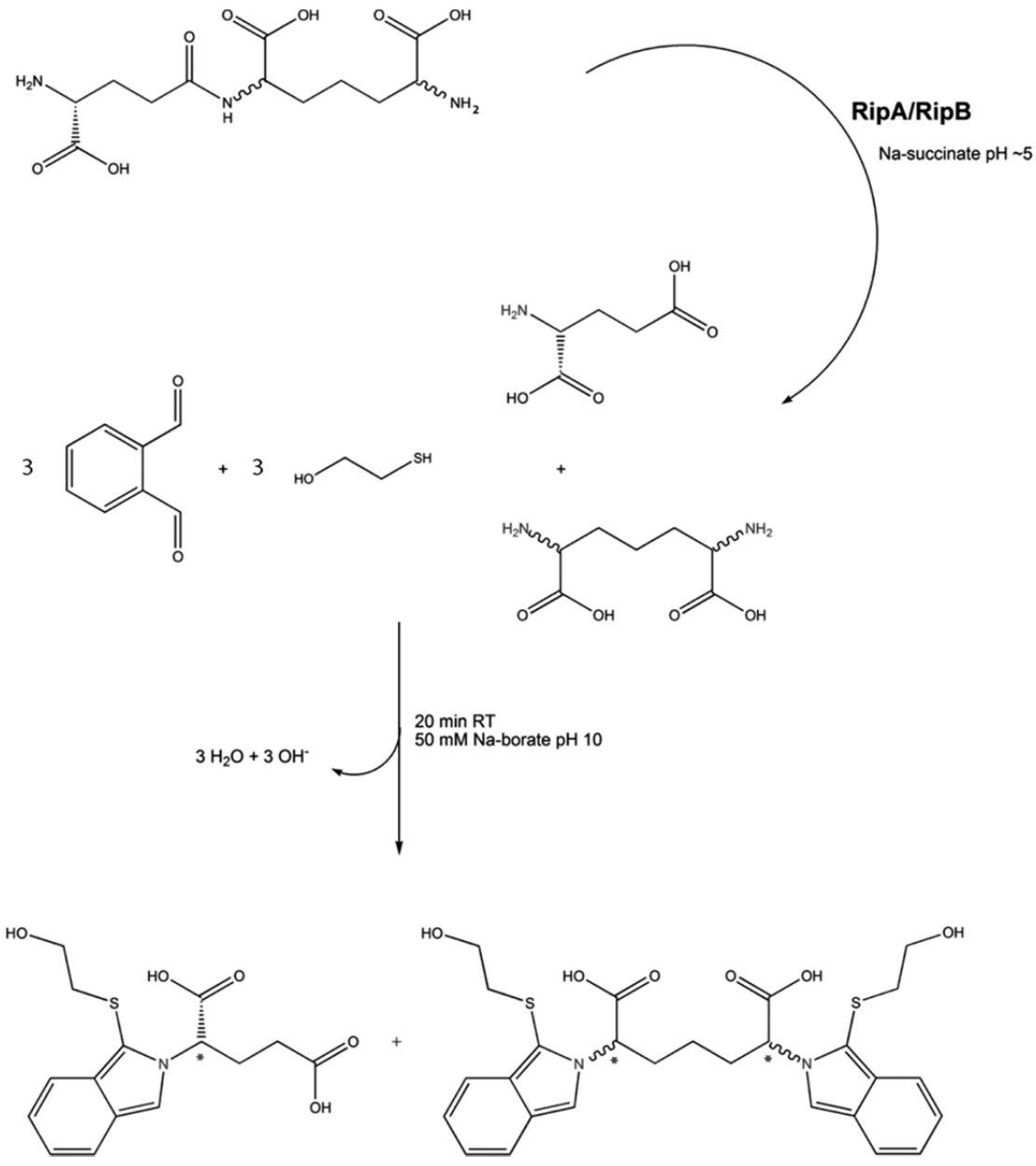

Figure 17: Reaction scheme following the formation of isoindole derivatives based on the catalytic activity of RipA and RipB. The enzymatic reaction is performed prior to the o-phthalaldehyde derivatization.

Full-length RipA and RipB were active on PG fragments as substrates *in vitro*. Similarly, RipA-NlpC/p60 (residues 260–472) showed activity on the PG fragments. After the assays were completed, full-length RipA, RipA-NlpC/p60 domain (residues 260–472) and RipB proteins were retained and tested for integrity by SDS-PAGE. No proteolytic cleavage of the proteins occurred during incubation and assays. These

findings suggest that the proteolytic removal of the N-terminal segment of RipA-NlpC/p60 (residues 263–283) suggested by others[157] is not necessary for catalytic activity and thus argues against an inhibitory role of this particular fragment.

The assay is based on a coupled reaction combining the enzymatic reaction to the synthesis of isoindole derivatives upon the reaction of o-phthalaldehyde with the primary amines of the product. This reaction can be monitored photometrically by which the readout can be directly related to the amount of primary amines in the sample.

High-molecular-weight (HMW) PG from *B. subtilis* has been used to further assess the hydrolase activity on the insoluble polymer. Interestingly, only RipA (C domain) showed a defined activity in the conditions tested in the experiment. HMW-PG from *Staphylococcus aureus* is not cleaved by the substrate-specific hydrolases of the NlpC/p60 protein RipA demonstrating substrate specificity towards PG similar to the mycobacterial substrate.

The 3D-structures of RipA (C-terminal domain; residues 260–472) and RipB (30–241) have been determined to 1.38 Å and 1.6 Å, respectively (Figure 18) (paper II). Both structures display the classical fold of NlpC/p60 proteins by a six stranded anti-parallel β-sheet packed against 3 α-helices. Both proteins show significant differences in the N-terminal segment of the respective protein construct (Figure 18 and 19). In RipB, this segment (residues 30–97) forms two α-helices, which clasp around the core. RipA displays a different feature, where the N-terminal segment forms in contrast a β-hairpin followed by a helical stretch (residues 260–321).

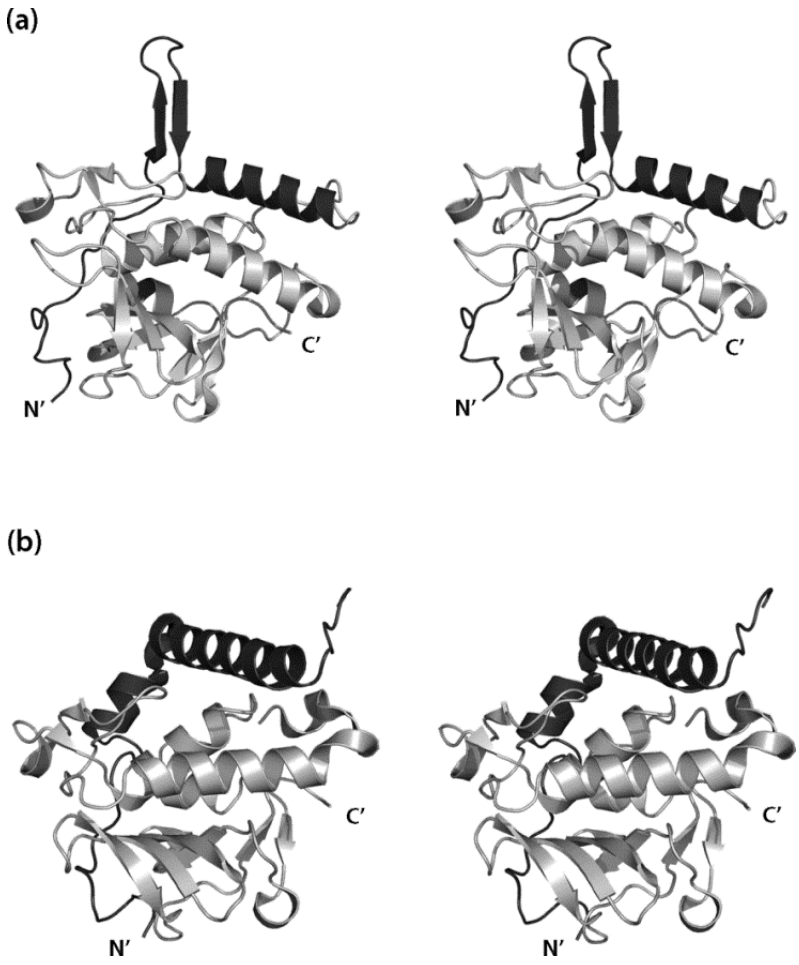

Figure 18: Stereo image of RipA (a) and RipB (b). Shown is the overall structure in cartoon representation. The catalytic NlpC/p60 domain is displayed in gray colour, the N-terminal segment in black.

The catalytic residues of the papain-like cysteine proteases are retained in RipA and RipB in similar 3D arrangement. Corresponding to Cys25, His159 and Asn175 in papain, RipB displays Cys152, His201 and Glu213 and RipA Cys383, His432 and Glu444. The active sites of RipA and RipB are shielded by the N-terminal segment, which falls back into the active site cleft. In the crystal structure, about 25 residues shield the binding groove for the incoming substrate (Figure 18). Probably, this segment adopts a different orientation in solution. Structural differences between RipA and RipB with respect to their N-terminal segments and surrounding of the binding groove could explain the differences in activity on HMW-PG.

Other members of the NlpC/p60 family display only 10-12% similarity to RipA and RipB. This is explained by the high variance in the N-terminal modules of the homologue proteins, which are often occurring. These N-terminal domains may direct their specific interaction with PG and possibly other cell wall components[160]

(Figure19). The *E. coli* enzyme Spr was the first which has been characterized as a NlpC/p60 protein, revealing the similarity to papain-type cysteine proteases[163]. Spr and RipD are the only available high resolution structures of NlpC/p60 proteins, which do not carry additional N-terminal extensions (Figure 19). The N-terminal segments of RipA and RipB are unique in the family of NlpC/p60 proteins. So far, only one structure of the *Bacillus cereus* YkfC NlpC/p60 family protein has been determined in complex with the PG-derived dipeptide L-alanyl-D-glutamic acid[164].

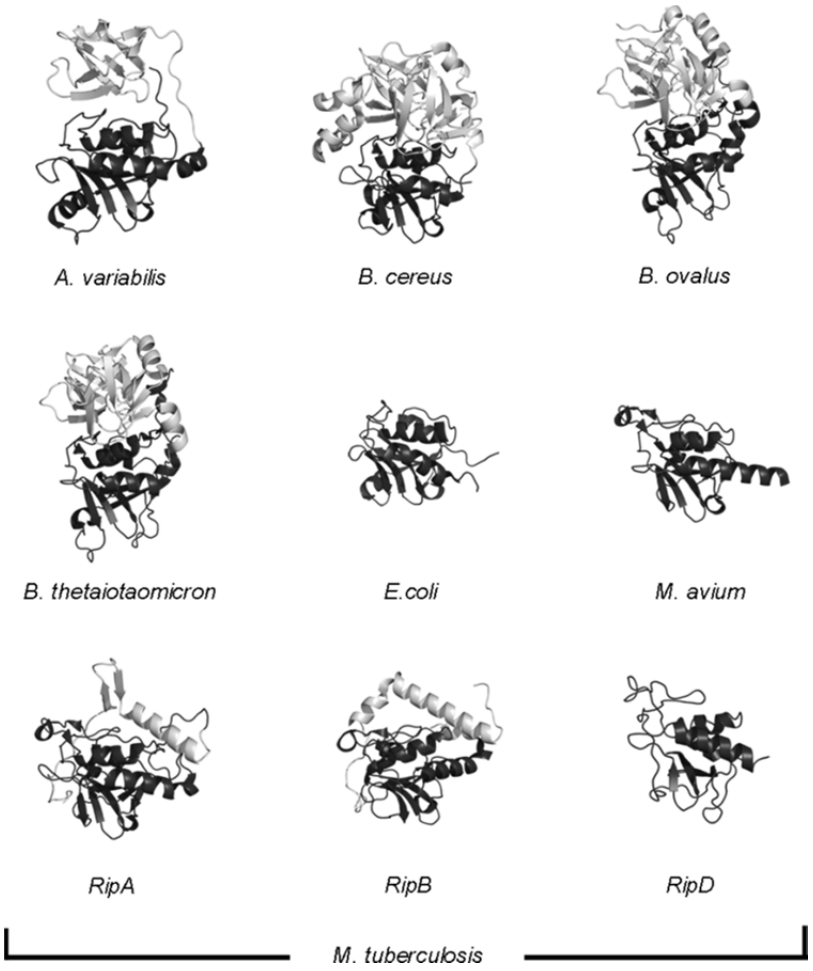

Figure 19: Domain organization of NlpC/p60 like proteins. The catalytic core is coloured in black, the variable N-terminal domains or smaller extensions are shown in gray.

3.4.4 RipD (Rv1566c), an NlpC/p60-like protein – *paper III*

RipD is an NlpC/p60 family protein encoded by the gene Rv1566c with about ~50% sequence similarity (residues 38–169) to the respective domains of RipA and RipB. In contrast to these NlpC/p60 proteases, the active site residues Cys383 and His432 are replaced in RipD by an alanine and a serine, respectively. A distinct C-terminal

pentapeptide (PVQQA)-repetitive extension protrudes from the NlpC/p60 core, which is unique for RipD homologues.

We determined the crystal structures of the core domain of RipD (residues 38–167) to 1.54 Å and a variant containing two pentarepeats to 1.2 Å resolution by molecular replacement using the homologue from *M. avium* as search model (PDB-ID:3GT2) (Figure 20).

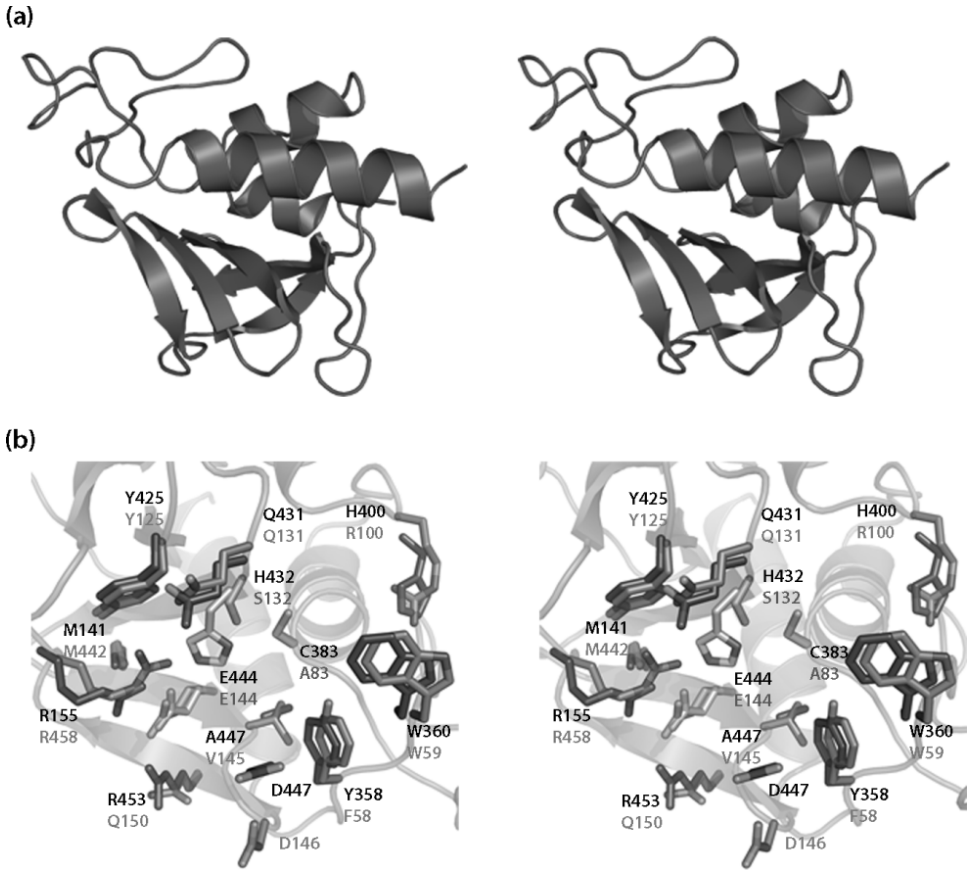

Figure 20: (a) Stereo-cartoon representation of RipD depicting the antiparallel β-sheet packed against 3 shorter α-helices common for NlpC/p60 proteins. (b) Superposition of RipA and RipD. Active site residues as well as surrounding residues are shown as gray (RipD) and black (RipA) sticks. The core domain in light gray shown in the background represents a cartoon of RipD.

Similarly to the homologues RipA and RipB in *M. tuberculosis*, the core domain of RipD folds in a five stranded anti-parallel β-sheet packed against three shorter α-helices. The structure of a related protein from *M. avium* has also been solved (PDB:3GT2, Ramyar et al., unpublished). The PG-binding in RipD is proposed to take place in an elongated groove similar to those found in RipA and RipB. Direct comparison of the full-length RipD (residues 38–230) comprising the pentapeptide repeat segment and the RipD core domain (residues 38–167) in solution by CD resulted

in an increase of random coil content, suggesting that the repeat does not adopt a defined secondary structure, which is a common property of perfect repeats.

In contrast to RipA and RipB, RipD does not show activity on PG fragments. However, the NlpC/p60 core domain retains the ability to bind PG as shown in paper III. This interaction is altered by the presence of the C-terminal pentapeptide repeat, rendering the full-length RipD less potent in binding to PG. In a binding experiment with isolated cell wall complex containing PG and arabinogalactan, the interaction was not altered suggesting no direct interaction with the arabinogalactan.

RipD-like proteins with amino acid replacements in the active site incompatible with catalysis are not very common. They are only found in mycobacterial genomes and closely related *Segniliparus ssp*. Interestingly, the occurrence of changes in the active site and C-terminal repeat is exceptional for mycobacterial species. In *M. smegmatis*, *M. abcessus*, *M gilvium* and *M. vanbaalenii* RipD-like proteins do not contain C-terminal repeats. Other cell envelope resident proteins have also been characterized carrying a proline-rich repeat e.g. the flagellar assembly protein of *Thiorhodococcus drewsii* or the heme exporter protein of *Yersinia spp*. Surprisingly, a mycobacteriophage protein also displaying a PVQXX repeat has been found[165].

We described RipD as an NlpC/p60 domain containing protein, which lost the catalytic activity to cleave the peptide stem of mycobacterial PG. The PG-binding however is retained and modulated by the presence of the C-terminal pentarepeat segment. RipD is the first example of an NlpC/p60 domain that evolved to a non-catalytic PG-binding protein. The 61 residue-long unstructured C-terminal pentapeptide repeat results in weaker interaction with PG *in vitro*, suggesting that the repeat segment modulates the RipD cell wall interaction. Possibly, the pentarepeat domain is involved in protein interaction between RipD and other periplasmic proteins or with other cell wall components[166].

Table 1: Occurrence of pentapeptide repeats in mycobacterial species and closely related *Segniliparus ssp.* The nature of the respective repeat domain is explicitly given.

Species (Strain)	Functional Annotation	Uniprot ID	Length (aa)	Repeat character N/L[¤]
M. tuberculosis (H37Rv)	invasion-associated protein	O06624	230	10/5
M. tuberculosis (H37Ra)[#]	putative invasion protein	A5U2S3	230	10/5
M. bovis (BCG and AF2122/97)	putative invasion protein	Q7VEY5	230	10/5
M. ulcerans (Agy99)	invasion protein	A0PNZ9	259	16/5
M. marinum (ATCC BAA-535)	invasion protein	B2HQ87	259	16/5
M. avium (k10)	hypothetical protein	Q740S0	316	19/5+3/4
M. avium (104)	NlpC/p60 protein	A0QHK2	289	21/5+3/4
M. leprae (TN)	secreted p60 protein	Q9CC67	212	1/5
M. abscessus (ATCC 19977)	hypothetical protein	B1MBD4	184	none
M. sp. (KMS and MCS)	NlpC/p60 protein	Q1B8K4	204	none
M. smegmatis (MC2 155)	putative invasion protein	A0QXZ3	220	none
M. gilvum (PYR-GCK)	NlpC/p60 protein	A4TAN6	214	none
M. vanbaalenii (PYR-1)	NlpC/p60 protein	A1T9C5	208	none
Segniliparus rotundus (DSM 44985)	NlpC/p60 protein	D6ZAC6	164	none
Segniliparus rugosus (ATCC BAA974)	NlpC/p60 protein	E5XV46	164	none

#… and other *M. tuberculosis* strains; RGTB327; RGTB423; F11; CDC1551; Haarlem (draft); strain C.
¤… N, number of repeats; L, length of one repeat unit

3.5 L,D-TRANSPEPTIDASES IN *M. TUBERCULOSIS*

Since *M. tuberculosis* expresses a significant number of class A lactamases[167], β-lactams were not considered as a promising medication against TB. However, a success in treatment of TB has revived the interest in a combination therapy with potent lactamase inhibitors of the clavulanate family and carbapenem-type β-lactams. A bactericidal effect has been proven, not only against growing *M. tuberculosis*, but also against the non-replicating forms[168]. Additionally, several of those combinations have shown to be active against XDR strains[167,168].

Carbapenem class β-lactams are active on transpeptidases necessary for the assembly of PG in the periplasmic space of *M. tuberculosis* and other species[152]. Two classes of transpeptidases have been described. D,D-transpeptidases of the penicillin-binding protein class necessary for the formation of 3-4 cross-links and L,D-transpeptidases, which link the peptide stems between the two adjacent Dap residues (3-3 cross-links). The 3-3 cross-link is the predominant form during the persistent state of *M. tuberculosis*[142,152]. L,D- and D,D-transpeptidases are structurally not related and function via a different catalytic mechanism[148,169].

The mycobacterial genome H37Rv encodes for the five homologs Ldt_{Mt1} to Ldt_{Mt5} of which Ldt_{Mt2} *(Rv2518c)* has been reported to be essential for virulence. Inactivation of the Ldt_{Mt2} gene leads to attenuation and increased susceptibility to clavulanate/lactam treatment *in vitro* and in mice[152]. All homologues of *M. tuberculosis* transpeptidases are susceptible to penem class β-lactams and these findings have triggered an interest in these enzymes in recent years. This is also reflected in crystal and NMR structures for L,D-transpeptidase from *M. tuberculosis* and other species being published by 5 different groups within a six months period[170–175]. Crystal structures of the enzyme with bound antibiotics are expected to open up the route for improved TB therapy[176] by providing templates for design of new inhibitors.

3.5.1 The structure of Ldt_{Mt2} – *paper IV*

Ldt_{Mt2} is a protein composed of a small intracellular segment (residues 1–17) followed by a transmembrane domain (residues 18–34) and a periplasmic part (residues 35–408). The catalytic domain (residues 250–408) could be well predicted from sequence alignment with homologues in *M. tuberculosis* and Corynebacterineae that also contain L,D-transpeptidases. We assessed the domain border of the residues 34(55)–250 by sequence comparisons to homologues, domain border prediction[177] and secondary structure prediction using Jpred[178] resulting in a predicted three domain organization, hereafter referred to as domain A, B and C (Figure 21). We cloned 13 and purified 10 constructs and were able to solve the crystal structure of the construct comprising the BC domain by Se-SAD phasing to 1.86 Å and subsequently the structure of the AB module by molecular replacement using the B domain of the BC module structure as a search model as described in paper IV (Figure 21). The BC module comprises the catalytic domain of the well characterized ErfK/YbiS/YhnG fold and an immunoglobulin (Ig)-like domain. The core of the transpeptidase domain folds into a β-sandwich formed by two anti-parallel β-sheets, which compares well to structure of the corresponding enzymes in *E. faecium* (PDB:1ZAT)[169] and *B. subtilis* (PDB:1Y7M)[179] with r.s.m.d. of 1.9 Å and 1.6 Å, respectively. The active site residues of Ldt_{Mt2} are Cys354 and His336 and correspond to Cys442 and His421 in the *E. faecium* homologue. A lid-like structure comprised of two anti-parallel β-strands closing the active site cleft by large aromatic residues of the lid (Tyr298, Tyr308, Tyr318) and of the core domain (Tyr330, Phe334 and Trp340).

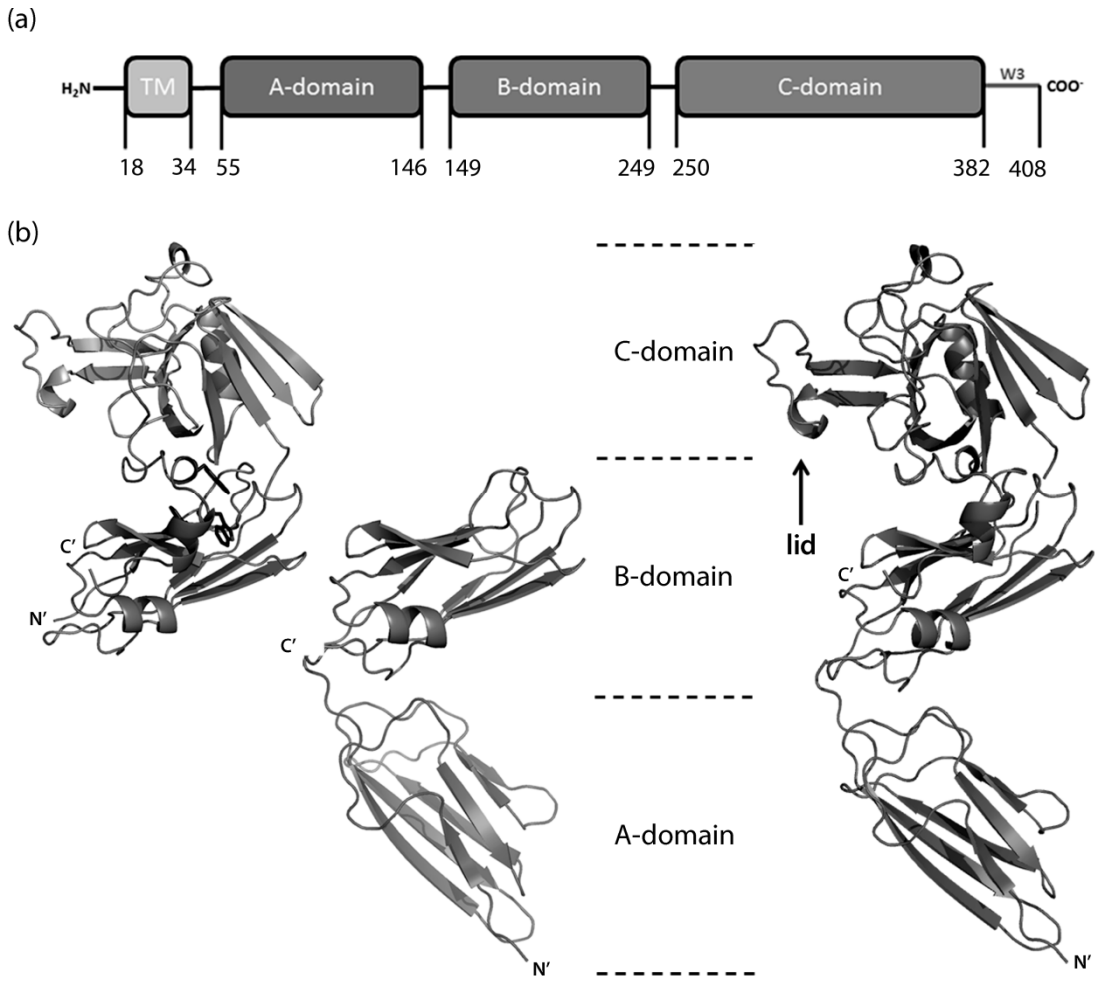

Figure 21: (a) Modular organization of Ldt_{Mt2} (Rv2518c). (b) Cartoon representation of the BC and the AB domain. (c) Reconstruction of the complete periplasmic part. Active site lid is indicated.

Both the A domain and the B domain have the same topology, corresponding to the c-type Ig fold. A structural alignment using the DALI algorithm revealed the closest structural homologous to be the periplasmic copper-resistance protein from *P. syringae* (PDB:2C9R)[180], the N-terminal domain of a amylase of *Halothermothrix orenii* (PDB:3BC9)[181] and a mannanase from *Cellolumonas fimi* (PDB:2X2Y)[182]. Functional relation to the copper-resistance protein is excluded since the copper-coordinating residues are missing. A relation to the other two proteins being involved in polysaccharide metabolism could be relevant due to the presence of glycans in the cell envelope of *M. tuberculosis* suggesting Ldt_{Mt2} is interacting with the glycan chains via the A and B domain. There are four surface-located threonine residues that are conserved between the amylase and the A domain of the Ldt_{Mt2}[181].

The extramembrane part of the Ldt_{Mt2} shows a three domain organization which we were able to reconstruct (Figure 21), whereas others missed one of the Ig domains[168].

Our model of the entire extramembrane part of the enzyme was confirmed by the structure determination of a three-domain construct comprising the A, B and C domains[174]. The three domain structure of Ldt_{Mt2} extends about 80 Å from the plasma membrane excluding a stretch of 20 missing amino acids at the N-terminus. This places the catalytic domain in a defined vicinity to the membrane. Interestingly, among the remaining four L,D-transpeptidases encoded in the mycobacterial genome Rv0116c Ldt_{Mt1} and Rv1433 contain only two domains, the C-terminal catalytic domain and the N-terminal Ig-like domain[183]. Both proteins show significant sequence identity to the BC domain of Ldt_{Mt2}. Rv0483 and Rv0192 have a three domain organization. They do not only show sequence identity to the BC domain, but also to the A domain (35% for Rv0483 and 18% for Rv0192).

Thus, two groups of L,D-transpeptidases are present in *M. tuberculosis*, those comprising three domains and those with two domains. Differences in the number of domains position the catalytically active C-terminal domains at different distances from the membrane and thereby follow the multilayered architecture of PG.

3.5.2 Ldt_{Mt2}-complex with β-lactam antibiotics

The formation of an acyl-enzyme complex between L,D-transpeptidases and β-lactams has been demonstrated with the homologue from *B. subtilis*[172]. We and others showed that Ldt_{Mt2} clearly interacts with penam and penem, cephalosporin class β-lactams[167,171].

Table 2: Covalent adducts formed with β-lactam type antibiotics imipenem and ampicillin.

Protein construct, MW (Da)	β-lactam, MW (Da)	Detected mass (Da)	Mass difference (Da)
Ldt_{Mt2} periplasmic segment (34-408) 40073.8	Imipenem, 299.3	40372.6	298.8
Ldt_{Mt2} BC-module (149-408), 28481.7	Imipenem, 299.3	28780.1	298.4
	Ampicillin, 349.4	28831.7	350.0

Development of carbapenems (penem class) for TB treatment has recently raised considerable interest since these drugs are uniformly active against MDR-TB and XDR-TB and kill both exponentially growing and dormant forms of the bacilli, in

association with the lactamase inhibitor clavulanic acid[168]. All five L,D-transpeptidases of *M. tuberculosis* have been tested for their activity in cross-linking PG peptide stems and for β-lactam acylation. The formation of the acyl-enzyme complex has been seen for all mycobacterial homologues Ldt_{Mt1-5}[171,176,184]. Crystal structures of Ldt_{Mt1} and Ldt_{Mt2} in complex with imipenem and meropenem, both members of the penem class of β-lactams, i.e. as the enzyme-acyl adduct, have been obtained. However, none of the adducts could be modeled completely due to missing electron density suggesting that large parts of the drugs are disordered in the binding site. This indicates that residues of the binding site do not significantly contribute to β-lactam selectivity. This conclusion is also strengthened by the formation of acyl-enzyme adducts with antibiotics of various β-lactam classes. In all these cases almost no interactions with the surrounding residues are present[173,183]. Nevertheless, based on the structural and biochemical information new lead compounds might be developed based on the core β-lactam scaffold.

3.6 TRAGETING THE CELL WALL – AN OUTLOOK

The importance of the cell wall makes it a well exploited target of a broad range of antibiotics. Potent inhibitors and first-line antibiotics have been developed such as INH, EMB, RIF and PYR, which target biosynthetic pathways of the mycobacterial cell wall. Currently, an emphasis is on the development for new alternatives of INH, an InhA inhibitor, which arrests mycolic acid synthesis. Recently, substituted triclosan derivatives have been shown to potently inhibit bacterial growth tested against INH-resistant strains of *M. tuberculosis*[185].

A second group of antimycobacterial drugs targeting the cell envelope are the arabinofuranosyltransferase inhibitors e.g. EMB. They disrupt the biosynthesis of AG and LAM and evoke an accumulation of β-D-arabinofuranosyl-P-decaprenol[186,187]. Here, EMB has also been used as a scaffold for the development of new anti-mycobacterial therapeutics. SQ09 has been synthesized as an analogue which displays promising pharmacokinetics, even in EMB-resistant strains[188]. Surprisingly, SQ09 does not inhibit the arabinosyltransferase, but rather a membrane transporter of TMM, MmpL3, preventing the incorporation of mycolic acids into the mycobacterial cell wall[189].

β-lactam antibiotics are probably the oldest group of antimicrobial drugs which have been administered during TB infection. Their prime target is the transpeptidase module

of penicillin binding proteins (PBPs), that cross-link PG subunits by D,D-transpeptidation, forming 3-4 linkages (DAP-D-Ala) that stabilise PG layer of the bacilli[149,190]. β-lactams mimic the newly formed peptide bond and are potent inhibitors counteracting the cross-link formation. This mechanism of attacking a key step in bacterial cell wall synthesis renders β-lactams a versatile class of antibiotics whose numerous members with various chemical and pharmacological properties exert bactericidal effects on a broad spectrum of bacterial pathogens.

However, there are two main reasons why β-lactam antibiotics have not been considered to be appropriate for the treatment of TB: *M. tuberculosis* produces a chromosomally encoded β-lactamase[167,191] and secondly, it has been shown that cross-links through 3,3-linkages (DAP-DAP) are of vast importance in mycobacterial PG[142,143]. These DAP-DAP linkages are produced by L,D-transpeptidases (Ldt_{Mt1} and Ldt_{Mt2}) rather than classical PBPs – a very different class of enzyme with a catalytic cysteine instead of a serine in the active site[152,171]. However the formation of the β-lactam acyl-enzyme complex has been shown for all mycobacterial homologues Ldt_{Mt1-5}[171,176,184]. Since the interaction is mainly driven by the covalent bond between drug and enzyme and not by the residues forming the surrounding of the active site, the rational design of new leads based on the β-lactam scaffold specific for L,D-transpeptidases is of high interest.

RipA has been identified as a potential drug target. A RipA knock-out showed a distinct phenotype rendering the bacilli with impaired growth and increased susceptibility towards ciprofloxacin, erythromycin and the first-line drug RIF[155]. According to the gene knock-out data, a potential inhibitor would probably be administered in a combination therapy regimen i.e. with RIF to successfully achieve bacterial clearance. The biochemical and biophysical characterization will guide the path towards the development of new inhibitors targeting RipA.

Taken together the efforts in characterizing new potential drug targets provide frameworks for a structure-based approach towards new leads against *M. tuberculosis*, which might be developed into new drug candidates.

4. ACKNOWLEDGEMENTS

My first word of gratitude goes to my main supervisor. Gunter, it was a great pleasure to have had you as a *Doktorvater* and I thank you that enough trust in me to take you into your group. You always guided me through these 4 years with excellent advice, both scientifically and personally. I am grateful that you always inspired me with your commitment to science. You are a source of great knowledge and I hope there are others to come to profit from your wisdom and mentorship.

Robert! What should I say? Micha sometimes called you "The Dark Lord", whose name shall not be mentioned … at home. You always kept me busy. And one thing I can tell you: you are the most German non-German I have ever come across – your drive for perfectionism and your pedagogical skills are remarkable. Your vast competence in many scientific disciplines is impressive. I learned so much from you and I could not have gotten a better co-supervisor. You even showed me the nicest castle in Sweden, what other boss would do that?

Ylva, you are my unofficial *Doktormutter*. You helped to provide a wonderful atmosphere in the lab and your competent input in crystallography was always valuable to me. I really admire your patience and ways of thinking. I am looking forward to have you as the chair of my defense.

I would like to express my deep gratitude to all the other members of the *Molekylär strukturbiologi*. Ahmad, you are a dear friend and the best lab manager one could imagine – I wish I could steal you away from Gunter and take you with me to Germany … *shall we*? ;) You organizational skills were invaluable for me and I doubt that I would have made it without your caring help. Good wishes also to your family. Eva and Katharina, you are my angels and my greatest source of support – our time together was something unique and it will forever have a special place in my heart – visit me as often as you can in Germany; I will miss you so much. Bernie and Doreen, my German anchors that always reminded me of what I missed so much in the last years: I thank you for the many hours in Hjulet that helped me to pass the lonely time at the beginning, all the invitations to your lovely home, the fantastic (!) food you prepared and all the help I got from you – both crystallographically as well as in private life!

Thank you for taking Micha as a student, you made my life more livable here. Ming Wei, I will always remember you for the following things: perfect body, war heads and a timeless sense of humor – I will visit you in Asia for sure. I wished we had had the time to also make me a body of steel. Jodie and Magnus, you are a dream team: I loved your helpful attitude, Jodie and I enjoyed the fruitful trips to ESRF together with you. I learned so much from you. Magnus – you will always be my office neighbor, thank you for three wonderful years. Edvard, I wished all Swedes could be like you – I remember you as one of the most helpful and kind persons I have encountered at KI. Maria, I admire your singing talents and it was a pleasure to be at your concerts. Domink, my namesake with a K, we started together and we had a great time in Fogdevreten, I wish you continued success. Ömer, I wish you all the best – you will have a great career.

Thanks to all the past members of MSB and the many other persons at MBB that made my life easier. Essam, your absence from Egypt is a loss for that country – thank you for letting me use the HPLC. I also thank all my other friends I made here such as Luise, Michael and Ylva! Rajesh, enjoy the beaches of Portugal!

A special thanks to all the friends I made outside KI that supported me so greatly, here this list should definitely be headed by Jenny, Laura and Håkan. You together with Eva and Katharina are very dear friends and I would not have survived the wilderness of Sweden without your loving help, your hospitality and the great great great time we spent together. We will forever stay in contact that is for sure and please, visit me often.

Ich danke meiner Familie, insbesondere meiner Mama und meinem Papa sowie meinen Geschwistern Daniel und Jannik für die Liebe und stete Unterstützung.

5. REFERENCES

1. Global Tuberculosis Report 2013. 1–97 (2013).

2. Fennelly, K. P. *et al.* Variability of infectious aerosols produced during coughing by patients with pulmonary tuberculosis. *Am. J. Respir. Crit. Care Med.* **186,** 450–7 (2012).

3. Garton, N. J. *et al.* Cytological and transcript analyses reveal fat and lazy persister-like bacilli in tuberculous sputum. *PLoS Med.* **5,** e75 (2008).

4. Pieters, J. Mycobacterium tuberculosis and the macrophage: maintaining a balance. *Cell Host Microbe* **3,** 399–407 (2008).

5. Grosset, J. Mycobacterium tuberculosis in the Extracellular Compartment: an Underestimated Adversary. *Antimicrob Agents Chemother* **47,** 833–836 (2003).

6. Chee, C. B.-E., Sester, M., Zhang, W. & Lange, C. Diagnosis and treatment of latent infection with Mycobacterium tuberculosis. *Respirology* **18,** 205–16 (2013).

7. Hernandez-Pando, R., Orozco, H. & Aguilar, D. Factors that deregulate the protective immune response in tuberculosis. *Arch. Immunol. Ther. Exp. (Warsz).* **57,** 355–67 (2009).

8. Gengenbacher, M. & Kaufmann, S. H. E. Mycobacterium tuberculosis: success through dormancy. *FEMS Microbiol. Rev.* **36,** 514–32 (2012).

9. Reece, S. T. & Kaufmann, S. H. E. Floating between the poles of pathology and protection: can we pin down the granuloma in tuberculosis? *Curr. Opin. Microbiol.* **15,** 63–70 (2012).

10. Rutledge, T. F. & Boyd, M. F. Updated Guidelines for Using Interferon Gamma Release Assays to Detect Mycobacterium tuberculosis Infection - United States , 2010. *Morb. Mortal. Wkly. Rep.* **59,** 1–25 (2010).

11. Zumla, A., Raviglione, M., Hafner, R. & von Reyn, C. F. Current Concepts - Tuberculosis. *N. Engl. J. Med.* **368,** 745–55 (2013).

12. Schlesinger, L. S., Azad, A. K., Torrelles, J. B. & Roberts, E. Determinants of Phagocytosis, Phagosome Biogenesis and Autophagy for Mycobacterium tuberculosis. *Handb. Tuberc. Immunol. Cell Biol.* 1–22 (2008).

13. Sturgill-Koszycki, S. *et al.* Lack of Acidification in Mycobacterium Phagosomes Produced by Exclusion of the Vesicular Proton-ATPase. *Science (80-.).* **263,** 678–681 (1994).

14. Eruslanov, E. B. *et al.* Neutrophil Responses to Mycobacterium tuberculosis Infection in Genetically Susceptible and Resistant Mice. *Infection* **73,** 1744–1753 (2005).

15. Wolf, A. J. *et al.* Mycobacterium tuberculosis Infects Dendritic Cells with High Frequency and Impairs Their Function In Vivo. *J. Immunol.* **179,** 2509–2519 (2007).

16. Lowe, D. M., Redford, P. S., Wilkinson, R. J., O'Garra, A. & Martineau, A. R. Neutrophils in tuberculosis: friend or foe? *Trends Immunol.* **33,** 14–25 (2012).

17. Fabri, M. *et al.* Vitamin D is required for IFN-gamma-mediated antimicrobial activity of human macrophages. *Sci. Transl. Med.* **3,** 104ra102 (2011).

18. Frieden, T. R., Sterling, T. R., Munsiff, S. S., Watt, C. J. & Dye, C. Tuberculosis. *Lancet* **362,** 887–99 (2003).

19. Kleinnijenhuis, J., Oosting, M., Joosten, L. a B., Netea, M. G. & Van Crevel, R. Innate immune recognition of Mycobacterium tuberculosis. *Clin. Dev. Immunol.* **2011,** 405310 (2011).

20. Keane, J., Remold, H. G. & Kornfeld, H. Virulent Mycobacterium tuberculosis strains evade apoptosis of infected alveolar macrophages. *J. Immunol.* **164,** 2016–20 (2000).

21. Kelly, D. M., ten Bokum, A. M. C., O'Leary, S. M., O'Sullivan, M. P. & Keane, J. Bystander macrophage apoptosis after Mycobacterium tuberculosis H37Ra infection. *Infect. Immun.* **76,** 351–60 (2008).

22. Liao, X. *et al.* Macrophage autophagy plays a protective role in advanced atherosclerosis. *Cell Metab.* **15,** 545–53 (2012).

23. Velmurugan, K. *et al.* Mycobacterium tuberculosis nuoG is a virulence gene that inhibits apoptosis of infected host cells. *PLoS Pathog.* **3,** e110 (2007).

24. Hinchey, J. *et al.* Enhanced priming of adaptive immunity by a proapoptotic mutant of Mycobacterium tuberculosis. *J. Clin. Invest.* **117,** 2279–2288 (2007).

25. Chen, M. *et al.* Lipid mediators in innate immunity against tuberculosis: opposing roles of PGE2 and LXA4 in the induction of macrophage death. *J. Exp. Med.* **205,** 2791–801 (2008).

26. Divangahi, M., Desjardins, D., Nunes-Alves, C., Remold, H. G. & Behar, S. M. Eicosanoid pathways regulate adaptive immunity to Mycobacterium tuberculosis. *Nat. Immunol.* **11,** 751–8 (2010).

27. O'Garra, A. *et al. The immune response in tuberculosis. Annu. Rev. Immunol.* **31,** 475–527 (2013).

28. Barry, C. E. *et al.* The spectrum of latent tuberculosis: rethinking the biology and intervention strategies. *Nat. Rev. Microbiol.* **7,** 845–55 (2009).

29. Russell, D. G., Cardona, P.-J., Kim, M.-J., Allain, S. & Altare, F. Foamy macrophages and the progression of the human tuberculosis granuloma. *Nat. Immunol.* **10,** 943–8 (2009).

30. Peters, W. & Ernst, J. D. Mechanisms of cell recruitment in the immune response to Mycobacterium tuberculosis. *Microbes Infect.* **5,** 151–8 (2003).

31. Tsai, M. C. *et al.* Characterization of the tuberculous granuloma in murine and human lungs: cellular composition and relative tissue oxygen tension. *Cell. Microbiol.* **8,** 218–32 (2006).

32. Warner, D. F. & Mizrahi, V. Complex genetics of drug resistance in Mycobacterium tuberculosis. *Nat. Genet.* **45,** 1107–8 (2013).

33. Zhang, H. *et al.* Genome sequencing of 161 Mycobacterium tuberculosis isolates from China identifies genes and intergenic regions associated with drug resistance. *Nat. Genet.* **45,** 1255–60 (2013).

34. Fox, W., Hutton, P. W., Sutherland, I. & Williams, a. W. A comparison of acute extensive pulmonary tuberculosis and its response to chemotherapy in Britain and Uganda. *Tubercle* **37,** 435–450 (1956).

35. Council, T. M. R. & Committee, T. B. T. A. R. Treatment of pulmonary tuberculosis with streptomycin and para-aminosalicylic acid. *Br Med* **2,** 1073–1085 (1950).

36. Mitchison, D. a. The diagnosis and therapy of tuberculosis during the past 100 years. *Am. J. Respir. Crit. Care Med.* **171,** 699–706 (2005).

37. Fox, W., Ellard, G. A. & Mitchison, D. A. Studies on the treatment of tuberculosis undertaken by the British Medical Research Council Tuberculosis Units, 1946-1986, with relevant subsequent publications. *Int. J. Tuberc. Lung Dis.* **3,** 231–279 (1999).

38. Mitchison, D. A. Prevention of Drug Resistance by Combined Drug Treatment of Tuberculosis. *Antibiot. Resist. Handb. Exp. Pharmacol.* **211,** 87–98 (2012).

39. Mitchison, D. A. How drug resistance emerges as a result of poor compliance during short course chemotherapy for tuberculosis Counterpoint. *Int. J. Tuberc. Lung Dis.* **2,** 10–15 (1998).

40. Vincent, V. *et al.* The TDR Tuberculosis Strain Bank: a resource for basic science, tool development and diagnostic services. *Int. J. Tuberc. Lung Dis.* **16,** 24–31 (2012).

41. Nathanson, C.-M. *et al.* The TDR Tuberculosis Specimen Bank: a resource for diagnostic test developers. *Int. J. Tuberc. Lung Dis.* **14,** 1461–7 (2010).

42. Jindani, A. & Griffin, G. E. Challenges to the development of new drugs and regimens for tuberculosis. *Tuberculosis (Edinb).* **90,** 168–70 (2010).

43. Via, L. E. *et al.* Tuberculous granulomas are hypoxic in guinea pigs, rabbits, and nonhuman primates. *Infect. Immun.* **76,** 2333–40 (2008).

44. Boshoff, H. I. M. *et al.* Biosynthesis and recycling of nicotinamide cofactors in mycobacterium tuberculosis. An essential role for NAD in nonreplicating bacilli. *J. Biol. Chem.* **283,** 19329–41 (2008).

45. Vilchèze, C. *et al.* Altered NADH/NAD+ Ratio Mediates Coresistance to Isoniazid and Ethionamide in Mycobacteria. *Antimicrob. Agents Chemother.* **49,** 708–720 (2005).

46. Trivedi, A., Singh, N., Bhat, S. A., Gupta, P. & Kumar, A. *Redox biology of tuberculosis pathogenesis. Adv. Microb. Physiol.* **60,** 263–324 (Elsevier Ltd., 2012).

47. Chan, E. D., Chan, J. & Schluger, N. W. What is the role of nitric oxide in murine and human host defense against tuberculosis? *Am. J. Respir. Cell Mol. Biol.* **25,** 606–12 (2001).

48. Winterbourn, C. C. The biological chemistry of hydrogen peroxide. *Methods Enzymol.* **528,** 3–25 (2013).

49. Kohanski, M. a, Dwyer, D. J., Hayete, B., Lawrence, C. a & Collins, J. J. A common mechanism of cellular death induced by bactericidal antibiotics. *Cell* **130,** 797–810 (2007).

50. Keren, I., Wu, Y., Inocencio, J., Mulcahy, L. R. & Lewis, K. Killing by bactericidal antibiotics does not depend on reactive oxygen species. *Science* **339,** 1213–6 (2013).

51. Liu, Y. & Imlay, J. A. Cell death from antibiotics without the involvement of reactive oxygen species. *Science* **75,** 5–19 (2013).

52. Cooper, A. M., Pearl, J. E., Brooks, J. V, Orme, I. M. & Ehlers, S. Expression of the Nitric Oxide Synthase 2 Gene Is Not Essential for Early Control of Mycobacterium tuberculosis in the Murine Lung. *Infect. Immun.* **68,** 6879–6882 (2000).

53. Adams, L. B., Dinauer, M. C., Morgenstern, D. E. & Krahenbuhl, J. L. Comparison of the roles of reactive oxygen and nitrogen intermediates in the host response to Mycobacterium tuberculosis using transgenic mice. *Tuber. Lung Dis.* **78,** 237–46 (1997).

54. Jung, Y.-J., LaCourse, R., Ryan, L. & North, R. J. Virulent but not Avirulent Mycobacterium tuberculosis Can Evade the Growth Inhibitory Action of a T Helper 1-dependent, Nitric Oxide Synthase 2-independent Defense in Mice. *J. Exp. Med.* **196,** 991–998 (2002).

55. Firmani, M. A. & Riley, L. W. Reactive Nitrogen Intermediates Have a Bacteriostatic Effect on Mycobacterium tuberculosis In Vitro. *J. Clin. Microbiol.* **40,** 1–6 (2002).

56. Chan, B. J., Xing, Y., Magliozzo, R. S. & Bloom, B. R. Killing of Virulent Mycobacterium tuberculosis by Reactive Nitrogen Intermediates Produced by Activated Murine Macrophages. *J. Exp. Med.* **175,** 1111–1122 (1992).

57. Nicholson, B. S. *et al.* Inducible Nitric Oxide Synthase in Pulmonary Alveolar Macrophages from Patients with Tuberculosis. *J. Exp. Med.* **183,** 2293–2302 (1996).

58. Roy, S., Sharma, S., Sharma, M., Aggarwal, R. & Bose, M. Induction of nitric oxide release from the human alveolar epithelial cell line A549: an in vitro correlate of innate immune response to Mycobacterium tuberculosis. *Immunology* **112,** 471–80 (2004).

59. Voskuil, M. I. *et al.* Inhibition of respiration by nitric oxide induces a Mycobacterium tuberculosis dormancy program. *J. Exp. Med.* **198,** 705–13 (2003).

60. Sherman, D. R. *et al.* Regulation of the Mycobacterium tuberculosis hypoxic response gene encoding alpha-crystallin. *Proc. Natl. Acad. Sci. U. S. A.* **98,** 7534–7539 (2001).

61. Boon, C. & Dick, T. Mycobacterium bovis BCG Response Regulator Essential for Hypoxic Dormancy. *J. Bacteriol.* **184,** 6760–6767 (2002).

62. Boon, C. & Dick, T. How Mycobacterium tuberculosis goes to sleep: the dormancy survival regulator DosR a decade later. *Futur. Microbiol.* **7,** 513–518 (2012).

63. Kumar, A. *et al.* Heme oxygenase-1-derived carbon monoxide induces the Mycobacterium tuberculosis dormancy regulon. *J. Biol. Chem.* **283,** 18032–9 (2008).

64. Shiloh, M. U., Manzanillo, P. & Cox, J. S. Mycobacterium tuberculosis senses host-derived carbon monoxide during macrophage infection. *Cell Host Microbe* **3,** 323–30 (2008).

65. Kumar, A., Toledo, J. C., Patel, R. P., Lancaster, J. R. & Steyn, A. J. C. Mycobacterium tuberculosis DosS is a redox sensor and DosT is a hypoxia sensor. *Proc. Natl. Acad. Sci. U. S. A.* **104,** 11568–73 (2007).

66. Honaker, R. W., Dhiman, R. K., Narayanasamy, P., Crick, D. C. & Voskuil, M. I. DosS responds to a reduced electron transport system to induce the Mycobacterium tuberculosis DosR regulon. *J. Bacteriol.* **192,** 6447–55 (2010).

67. Jakimowicz, P. *et al.* Evidence that the Streptomyces developmental protein WhiD, a member of the WhiB family, binds a [4Fe-4S] cluster. *J. Biol. Chem.* **280,** 8309–15 (2005).

68. Singh, A. *et al.* Mycobacterium tuberculosis WhiB3 responds to O2 and nitric oxide via its [4Fe-4S] cluster and is essential for nutrient starvation survival. *Proc. Natl. Acad. Sci. U. S. A.* **104,** 11562–7 (2007).

69. Paget, M. S. B. & Buttner, M. J. Thiol-based regulatory switches. *Annu. Rev. Genet.* **37,** 91–121 (2003).

70. Bornemann, C., Jardine, M. A., Spies, H. S. C. & Steenkamp, D. J. Biosynthesis of mycothiol: elucidation of the sequence of steps in Mycobacterium smegmatis. *Biochem J.* **325,** 623–629 (1997).

71. Rawat, M. *et al.* Mycothiol-Deficient Mycobacterium smegmatis Mutants Are Hypersensitive to Alkylating Agents, Free Radicals, and Antibiotics. *Antimicrob. Agents Chemother.* **46,** 3348–3355 (2002).

72. Ung, K. S. E. & Av-Gay, Y. Mycothiol-dependent mycobacterial response to oxidative stress. *FEBS Lett.* **580,** 2712–6 (2006).

73. Ordóñez, E. *et al.* Arsenate reductase, mycothiol, and mycoredoxin concert thiol/disulfide exchange. *J. Biol. Chem.* **284,** 15107–16 (2009).

74. Koledin, T., Newton, G. L. & Fahey, R. C. Identification of the mycothiol synthase gene (mshD) encoding the acetyltransferase producing mycothiol in actinomycetes. *Arch. Microbiol.* **178,** 331–7 (2002).

75. Gutierrez-Lugo, M.-T., Baker, H., Shiloach, J., Boshoff, H. & Bewley, C. a. Dequalinium, a new inhibitor of Mycobacterium tuberculosis mycothiol ligase identified by high-throughput screening. *J. Biomol. Screen.* **14,** 643–52 (2009).

76. Newton, G. L., Buchmeier, N., La Clair, J. J. & Fahey, R. C. Evaluation of NTF1836 as an inhibitor of the mycothiol biosynthetic enzyme MshC in growing and non-replicating Mycobacterium tuberculosis. *Bioorg. Med. Chem.* **19,** 3956–64 (2011).

77. Seebeck, F. P. In vitro reconstitution of Mycobacterial ergothioneine biosynthesis. *J. Am. Chem. Soc.* **132,** 6632–3 (2010).

78. Ta, P., Buchmeier, N., Newton, G. L., Rawat, M. & Fahey, R. C. Organic hydroperoxide resistance protein and ergothioneine compensate for loss of mycothiol in Mycobacterium smegmatis mutants. *J. Bacteriol.* **193,** 1981–90 (2011).

79. Kadokura, H., Katzen, F. & Beckwith, J. Protein disulfide bond formation in prokaryotes. *Annu. Rev. Biochem.* **72,** 111–35 (2003).

80. Martin, J. L. Thioredoxin - a fold for all reasons. *Structure* **3,** 245–50 (1995).

81. Williams, C. H. Mechanism and structure of thioredoxin reductase from Escherichia coli. *FASEB J.* **9,** 1267–1276 (1995).

82. Akif, M., Khare, G., Tyagi, A. K., Mande, S. C. & Sardesai, A. a. Functional studies of multiple thioredoxins from Mycobacterium tuberculosis. *J. Bacteriol.* **190,** 7087–95 (2008).

83. Sassetti, C. M., Boyd, D. H. & Rubin, E. J. Genes required for mycobacterial growth defined by high density mutagenesis. *Mol. Microbiol.* **48,** 77–84 (2003).

84. Akif, M., Suhre, K., Verma, C. & Mande, S. C. Conformational flexibility of Mycobacterium tuberculosis thioredoxin reductase: crystal structure and normal-mode analysis. *Acta Crystallogr. D. Biol. Crystallogr.* **61,** 1603–11 (2005).

85. Rhee, S. G., Chae, H. Z. & Kim, K. Peroxiredoxins: a historical overview and speculative preview of novel mechanisms and emerging concepts in cell signaling. *Free Radic. Biol. Med.* **38,** 1543–52 (2005).

86. Kalinina, E. V, Chernov, N. N. & Saprin, a N. Involvement of thio-, peroxi-, and glutaredoxins in cellular redox-dependent processes. *Biochem. Biokhimiia* **73,** 1493–510 (2008).

87. Hu, Y. & Coates, A. R. M. Increased levels of sigJ mRNA in late stationary phase cultures of Mycobacterium tuberculosis detected by DNA array hybridisation. *FEMS Microbiol. Lett.* **202,** 59–65 (2001).

88. Schnappinger, D. *et al.* Transcriptional Adaptation of Mycobacterium tuberculosis within Macrophages: Insights into the Phagosomal Environment. *J. Exp. Med.* **198,** 693–704 (2003).

89. Hampshire, T. *et al.* Stationary phase gene expression of Mycobacterium tuberculosis following a progressive nutrient depletion: a model for persistent organisms? *Tuberculosis (Edinb).* **84,** 228–38 (2004).

90. Rengarajan, J., Bloom, B. R. & Rubin, E. J. Genome-wide requirements for Mycobacterium tuberculosis adaptation and survival in macrophages. *Proc. Natl. Acad. Sci. U. S. A.* **102,** 8327–32 (2005).

91. Hatzios, S. K. & Bertozzi, C. R. The regulation of sulfur metabolism in Mycobacterium tuberculosis. *PLoS Pathog.* **7,** e1002036 (2011).

92. Schelle, M. W. & Bertozzi, C. R. Sulfate metabolism in mycobacteria. *Chembiochem* **7,** 1516–24 (2006).

93. Carroll, K. S. *et al.* A conserved mechanism for sulfonucleotide reduction. *PLoS Biol.* **3,** e250 (2005).

94. Mougous, J. D. *et al.* A sulfated metabolite produced by stf3 negatively regulates the virulence of Mycobacterium tuberculosis. *Proc. Natl. Acad. Sci. U. S. A.* **103,** 4258–63 (2006).

95. Schnell, R., Sandalova, T., Hellman, U., Lindqvist, Y. & Schneider, G. Siroheme- and [Fe4-S4]-dependent NirA from Mycobacterium tuberculosis is a sulfite reductase with a covalent Cys-Tyr bond in the active site. *J. Biol. Chem.* **280,** 27319–28 (2005).

96. Schnell, R., Oehlmann, W., Singh, M. & Schneider, G. Structural insights into catalysis and inhibition of O-acetylserine sulfhydrylase from Mycobacterium tuberculosis. Crystal structures of the enzyme alpha-aminoacrylate intermediate and an enzyme-inhibitor complex. *J. Biol. Chem.* **282,** 23473–81 (2007).

97. Agren, D., Schnell, R., Oehlmann, W., Singh, M. & Schneider, G. Cysteine synthase (CysM) of Mycobacterium tuberculosis is an O-phosphoserine sulfhydrylase: evidence for an alternative cysteine biosynthesis pathway in mycobacteria. *J. Biol. Chem.* **283,** 31567–74 (2008).

98. Qiu, J., Wang, D., Ma, Y., Jiang, T. & Xin, Y. Identification and characterization of serine acetyltransferase encoded by the Mycobacterium tuberculosis Rv2335 gene. *Int. J. Mol. Med.* **31,** 1229–33 (2013).

99. O'Leary, S. E., Jurgenson, C. T., Ealick, S. E. & Begley, T. P. O-phospho-L-serine and the thiocarboxylated sulfur carrier protein CysO-COSH are substrates for CysM, a cysteine synthase from Mycobacterium tuberculosis. *Biochemistry* **47,** 11606–15 (2008).

100. Agren, D., Schnell, R. & Schneider, G. The C-terminal of CysM from Mycobacterium tuberculosis protects the aminoacrylate intermediate and is involved in sulfur donor selectivity. *FEBS Lett.* **583,** 330–6 (2009).

101. Schnell, R. & Schneider, G. Structural enzymology of sulphur metabolism in Mycobacterium tuberculosis. *Biochem. Biophys. Res. Commun.* **396,** 33–8 (2010).

102. Huang, B., Vetting, M. W. & Roderick, S. L. The Active Site of O-Acetylserine Sulfhydrylase Is the Anchor Point for Bienzyme Complex Formation with Serine Acetyltransferase. *J. Bacteriol.* **187,** 3201–3205 (2005).

103. Bonner, E. R., Cahoon, R. E., Knapke, S. M. & Jez, J. M. Molecular basis of cysteine biosynthesis in plants: structural and functional analysis of O-acetylserine sulfhydrylase from Arabidopsis thaliana. *J. Biol. Chem.* **280,** 38803–13 (2005).

104. Mino, K. *et al.* Characteristics of Serine Acetyltransferase from Escherichia coli Deleting Different Lengths of Amino Acid Residues from the C-Terminus. *Biosci. Biotechnol. Biochem.* **64,** 1874–1880 (2000).

105. Jean Kumar, V. U. *et al.* Discovery of novel inhibitors targeting the Mycobacterium tuberculosis O-acetylserine sulfhydrylase (CysK1) using virtual high-throughput screening. *Bioorg. Med. Chem. Lett.* **23,** 1182–6 (2013).

106. Poyraz, O. *et al.* Structure-guided design of novel thiazolidine inhibitors of O-acetyl serine sulfhydrylase from Mycobacterium tuberculosis. *J. Med. Chem.* **56,** 6457–66 (2013).

107. Jurgenson, C. T., Burns, K. E., Begley, T. P. & Ealick, S. E. Crystal structure of a sulfur carrier protein complex found in the cysteine biosynthetic pathway of Mycobacterium tuberculosis. *Biochemistry* **47,** 10354–64 (2008).

108. Schneider, G., Käck, H. & Lindqvist, Y. The manifold of vitamin B6 dependent enzymes. *Structure* **8,** R1–6 (2000).

109. Burns, K. E. *et al.* Reconstitution of a new cysteine biosynthetic pathway in Mycobacterium tuberculosis. *J. Am. Chem. Soc.* **127,** 11602–3 (2005).

110. Karsten, W. E. & Cook, P. F. Detection of intermediates in reactions catalyzed by PLP-dependent enzymes: O-acetylserine sulfhydrylase and serine-glyoxalate aminotransferase. *Methods Enzymol.* **354,** 223–237 (2002).

111. Schnackerz, K. D., Ehrlich, J. H., Giesemann, W. & Reed, T. a. Mechanism of action of D-serine dehydratase. Identification of a transient intermediate. *Biochemistry* **18,** 3557–63 (1979).

112. Gaitonde, M. K. A spectrophotometric method for the direct determination of cysteine in the presence of other naturally occurring amino acids. *Biochem. J.* **104,** 627–33 (1967).

113. Kaur, D., Guerin, M. E., Skovierová, H., Brennan, P. J. & Jackson, M. Chapter 2: Biogenesis of the cell wall and other glycoconjugates of Mycobacterium tuberculosis. *Adv. Appl. Microbiol.* **69,** 23–78 (2009).

114. Zuber, B. *et al.* Direct visualization of the outer membrane of mycobacteria and corynebacteria in their native state. *J. Bacteriol.* **190,** 5672–80 (2008).

115. Hoffmann, C., Leis, A., Niederweis, M., Plitzko, J. M. & Engelhardt, H. Disclosure of the mycobacterial outer membrane: cryo-electron tomography and vitreous sections reveal the lipid bilayer structure. *Proc. Natl. Acad. Sci. U. S. A.* **105,** 3963–7 (2008).

116. Hett, E. C., Chao, M. C., Deng, L. L. & Rubin, E. J. A Mycobacterial Enzyme Essential for Cell Division Synergizes with Resuscitation-Promoting Factor. *PLoS Pathog* **4,** (2008).

117. Hett, E. C. & Rubin, E. J. Bacterial growth and cell division: a mycobacterial perspective. *Microbiol. Mol. Biol. Rev.* **72,** 126–56, table of contents (2008).

118. Chapman, G. B., Hanks, J. H. & Wallace, J. H. An electron microscope study of the disposition and fine structure of Mycobacterium lepraemurium in mouse spleen. *J. Bacteriol.* **77,** 205–11 (1959).

119. Schwebach, J. R. *et al.* Glucan Is a Component of the Mycobacterium tuberculosis Surface That Is Expressed In Vitro and In Vivo Glucan Is a Component of the Mycobacterium tuberculosis Surface That Is Expressed In Vitro and In Vivo. *Infect. Immun.* **70,** 2566–2575 (2002).

120. Lemassu, A. & Daffé, M. Structural features of the exocellular polysaccharides of Mycobacterium tuberculosis. *Biochem. J.* **297,** 351–7 (1994).

121. Ortalo-Magné, A. *et al.* Molecular composition of the outermost capsular material of the tubercle bacillus. *Microbiology* **141,** 1609–20 (1995).

122. Dinadayala, P. *et al.* Revisiting the structure of the anti-neoplastic glucans of Mycobacterium bovis Bacille Calmette-Guerin. Structural analysis of the extracellular and boiling water extract-derived glucans of the vaccine substrains. *J. Biol. Chem.* **279,** 12369–78 (2004).

123. Sambou, T. *et al.* Capsular glucan and intracellular glycogen of Mycobacterium tuberculosis: biosynthesis and impact on the persistence in mice. *Mol. Microbiol.* **70,** 762–74 (2008).

124. Mishra, A. K., Driessen, N. N., Appelmelk, B. J. & Besra, G. S. Lipoarabinomannan and related glycoconjugates: structure, biogenesis and role in Mycobacterium tuberculosis physiology and host-pathogen interaction. *FEMS Microbiol. Rev.* **35,** 1126–57 (2011).

125. Ballou, C. E. & Lee, Y. C. The Structure of a Myoinositol Mannoside from Mycobacterium tuberculosis Glycolipid. *Biochemistry* **3,** 682–685 (1964).

126. Chatterjee, D. & Khoo, K. H. Mycobacterial lipoarabinomannan: an extraordinary lipoheteroglycan with profound physiological effects. *Glycobiology* **8,** 113–20 (1998).

127. Nigou, J. & Besra, G. S. Cytidine diphosphate-diacylglycerol synthesis in Mycobacterium smegmatis. *Biochem. J.* **367,** 157–62 (2002).

128. Hunter, S. W., Gaylord, H. & Brennan, P. J. Structure and antigenicity of the phosphorylated lipopolysaccharide antigens from the leprosy and tubercle bacilli. *J. Biol. Chem.* **261,** 12345–51 (1986).

129. Chatterjee, D., Bozic, C. M., McNeil, M. & Brennan, P. J. Structural features of the arabinan component of the lipoarabinomannan of Mycobacterium tuberculosis. *J. Biol. Chem.* **266,** 9652–60 (1991).

130. Khoo, K.-H., Dell, A., Morris, H. R., Brennan, P. J. & Chatterjee, D. Inositol Phosphate Capping of the Nonreducing Termini of Lipoarabinomannan from Rapidly Growing Strains of Mycobacterium. *J. Biol. Chem.* **270,** 12380–12389 (1995).

131. Vergne, I., Chua, J., Singh, S. B. & Deretic, V. Cell biology of mycobacterium tuberculosis phagosome. *Annu. Rev. Cell Dev. Biol.* **20,** 367–94 (2004).

132. Peng, W., Zou, L., Bhamidi, S., McNeil, M. R. & Lowary, T. L. The galactosamine residue in mycobacterial arabinogalactan is α-linked. *J. Org. Chem.* **77,** 9826–32 (2012).

133. Crick, D. C., Mahapatra, S. & Brennan, P. J. Biosynthesis of the arabinogalactan-peptidoglycan complex of Mycobacterium tuberculosis. *Glycobiology* **11,** 107R–118R (2001).

134. Vollmer, W., Blanot, D. & Pedro, M. A. De. Peptidoglycan structure and architecture. *FEMS Microbiol. Rev.* **32,** 149–167 (2008).

135. Vollmer, W., Höltje, J. & Ho, J. The Architecture of the Murein (Peptidoglycan) in Gram-Negative Bacteria: Vertical Scaffold or Horizontal Layer(s)? *J. Bacteriol.* **186,** 5978–5987 (2004).

136. Meroueh, S. O. *et al.* Three-dimensional structure of the bacterial cell wall peptidoglycan. *Proc. Natl. Acad. Sci. U. S. A.* **103,** 4404–9 (2006).

137. Schleifer, K. H. & Kandler, O. Peptidoglycan types of bacterial cell walls and their taxonomic implications. *Bacteriol. Rev.* **36,** 407–77 (1972).

138. Mahapatra, S., Scherman, H., Patrick, J., Crick, D. C. & Brennan, P. J. N-Glycolylation of the Nucleotide Precursors of Peptidoglycan Biosynthesis of Mycobacterium spp. Is Altered by Drug Treatment. *J. Bacteriol.* **187,** 2341–2347 (2005).

139. Raymond, J. B., Mahapatra, S., Crick, C., Pavelka, M. S. & Crick, D. C. Glycobiology and Extracellular Matrices: Identification of the namH Gene, Encoding the Hydroxylase Responsible for the N-Glycolylation of the Mycobacterial Peptidoglycan. *J. Biol. Chem.* **280,** 326–333 (2005).

140. Raymond, J. B., Mahapatra, S., Crick, D. C. & Pavelka, M. S. Identification of the namH gene, encoding the hydroxylase responsible for the N-glycolylation of the mycobacterial peptidoglycan. *J. Biol. Chem.* **280,** 326–33 (2005).

141. Vollmer, W., Joris, B., Charlier, P. & Foster, S. Bacterial peptidoglycan (murein) hydrolases. **32,** 259–86 (2008).

142. Lavollay, M. *et al.* The peptidoglycan of stationary-phase Mycobacterium tuberculosis predominantly contains cross-links generated by L,D-transpeptidation. *J. Bacteriol.* **190,** 4360–6 (2008).

143. Wietzerbin, J. *et al.* Occurrence of D-Alanyl-(D)-meso-diaminopimelic Acid and meso-Diaminopimelyl-meso-diaminopimelic Acid Interpeptide Linkages in the Peptidoglycan of Mycobacteria. *Biochemistry* **13,** 3471–3476 (1984).

144. Typas, A., Banzhaf, M., Gross, C. A. & Vollmer, W. From the regulation of peptidoglycan synthesis to bacterial growth and morphology. *Nat. Publ. Gr.* **10,** 123–136 (2011).

145. Barreteau, H. *et al.* Cytoplasmic steps of peptidoglycan biosynthesis. *FEMS Microbiol. Rev.* **32,** 168–207 (2008).

146. Bouhss, A., Trunkfield, A. E., Bugg, T. D. H. & Mengin-lecreulx, D. The biosynthesis of peptidoglycan lipid-linked intermediates. *FEMS Microbiol. Rev.* **32,** 208–233 (2008).

147. Mohammadi, T. *et al.* Identification of FtsW as a transporter of lipid- linked cell wall precursors across the membrane. *EMBO J.* **30,** 1425–1432 (2011).

148. Mainardi, J. *et al.* A Novel Peptidoglycan Cross-linking Enzyme for β-Lactam-resistant Transpeptidation Pathway. *J. Biol. Chem.* **280,** 38146–38152 (2005).

149. Goffin, C. & Ghuysen, J. Multimodular Penicillin-Binding Proteins: An Enigmatic Family of Orthologs and Paralogs. *Microbiol. Mol. Biol. Rev.* **62,** 1079–1093 (1998).

150. Chambers, H. F. *et al.* Can penicillins and other β-lactam antibiotics be used to treat tuberculosis? *Antimicrob. Agents Chemother.* **39,** 2620–2624 (1995).

151. Triboulet, S. *et al.* Inactivation Kinetics of a New Target of β-Lactam Antibiotics. *J. Biol. Chem.* **286,** 22777–22784 (2011).

152. Gupta, R. *et al.* The Mycobacterium tuberculosis protein Ldt Mt2 is a nonclassical transpeptidase required for virulence and resistance to amoxicillin. *Nat. Med.* **16,** 466–469 (2010).

153. Kana, B. D. *et al.* The resuscitation-promoting factors of Mycobacterium tuberculosis are required for virulence and resuscitation from dormancy but are collectively dispensable for growth in vitro. *Mol. Microbiol.* **67,** 672–84 (2008).

154. Mellroth, P., Karlsson, J. & Steiner, H. A scavenger function for a Drosophila peptidoglycan recognition protein. *J. Biol. Chem.* **278,** 7059–64 (2003).

155. Gao, L., Pak, M., Kish, R., Kajihara, K. & Brown, E. J. A Mycobacterial Operon Essential for Virulence In Vivo and Invasion and Intracellular Persistence in Macrophages A Mycobacterial Operon Essential for Virulence In Vivo and Invasion and Intracellular Persistence in Macrophages. *Infect. Immun.* **74,** 1757–1767 (2006).

156. Böth, D., Schneider, G. & Schnell, R. Peptidoglycan remodeling in Mycobacterium tuberculosis: comparison of structures and catalytic activities of RipA and RipB. *J. Mol. Biol.* **413,** 247–260 (2011).

157. Ruggiero, A. *et al.* Structure and functional regulation of RipA, a mycobacterial enzyme essential for daughter cell separation. *Structure* **18,** 1184–1190 (2010).

158. Boudreau, M. A., Fisher, J. F. & Mobashery, S. Messenger Functions of the Bacterial Cell Wall-derived Muropeptides. *Biochemistry* **51,** 2974−2990 (2012).

159. Ohnishi, R., Ishikawa, S. & Sekiguchi, J. Peptidoglycan Hydrolase LytF Plays a Role in Cell Separation with CwlF during Vegetative Growth of Bacillus subtilis These include : Peptidoglycan Hydrolase LytF Plays a Role in Cell Separation with CwlF during Vegetative Growth of Bacillus subtilis. *J. Bacteriol.* **181,** 1–8 (1999).

160. Anantharaman, V. & Aravind, L. Evolutionary history, structural features and biochemical diversity of the NlpC/P60 superfamily of enzymes. *Genome Biol.* **4,** R11 (2003).

161. Kana, B. D. & Mizrahi, V. Resuscitation-promoting factors as lytic enzymes for bacterial growth and signaling. *FEMS Immunol Med Microbiol* **58,** 39–50 (2010).

162. Hett, E. C., Chao, M. C. & Rubin, E. J. Interaction and Modulation of Two Antagonistic Cell Wall Enzymes of Mycobacteria. *PLoS Pathog.* **6,** 1–14 (2010).

163. Aramini, J. M. *et al.* Solution NMR structure of the NlpC/P60 domain of lipoprotein Spr from Escherichia coli: structural evidence for a novel cysteine peptidase catalytic triad. *Biochemistry* **47,** 9715–7 (2008).

164. Xu, Q. & Abdubeck, P. Structure of the c-D-glutamyl-L-diamino acid endopeptidase YkfC from Bacillus cereus in complex with L-Ala-c-D-Glu: insights into substrate recognition by NlpC/P60 cysteine peptidases. *Acta Crystallogr. Sect. F. Struct. Biol. Cryst. Commun.* **F66,** 1354–1364 (2010).

165. Pope, W. H. *et al.* Cluster K mycobacteriophages: insights into the evolutionary origins of mycobacteriophage TM4. *PLoS One* **6,** e26750 (2011).

166. Böth, D., Steiner, E. M., Izumi, A., Schneider, G. & Schnell, R. RipD (Rv1566c) from Mycobacterium tuberculosis: adaptation of an NlpC/p60 domain to a non-catalytic peptidoglycan-binding function. *Biochem J.* 1–21 (2013).

167. Hugonnet, J. & Blanchard, J. S. Irreversible Inhibition of the Mycobacterium tuberculosis -Lactamase by Clavulanate. *Biochemistry* **46,** 11998–12004 (2007).

168. Hugonnet, J.-E., Tremblay, L. W., Boshoff, H. I., Barry, C. E. & Blanchard, J. S. Meropenem-Clavulanate Is Effective Against Extensively Drug-Resistant Mycobacterium tuberculosis. *Science (80-.).* **33,** 1215–1218 (2009).

169. Biarrotte-sorin, S. *et al.* Crystal Structure of a Novel β-Lactam-insensitive Peptidoglycan Transpeptidase. *J. Mol. Biol.* **359,** 533–538 (2006).

170. Erdemli, S. B. *et al.* Targeting the cell wall of Mycobacterium tuberculosis: structure and mechanism of L,D-transpeptidase 2. *Structure* **20,** 2103–15 (2012).

171. Böth, D. *et al.* Structure of LdtMt2, an L,D-transpeptidase from Mycobacterium tuberculosis. *Acta Crystallogr. D. Biol. Crystallogr.* **69,** 432–41 (2013).

172. Lecoq, L. *et al.* Dynamics Induced by β-Lactam Antibiotics in the Active Site of Bacillus subtilis L,D-Transpeptidase. *Structure* **20,** 850–861 (2012).

173. Kim, H. S. *et al.* Structural basis for the inhibition of Mycobacterium tuberculosis L,D-transpeptidase by meropenem, a drug effective against extensively drug-resistant strains. *Acta Crystallogr. D. Biol. Crystallogr.* **69,** 420–31 (2013).

174. Li, W.-J. *et al.* Crystal structure of L,D-transpeptidase LdtMt2 in complex with meropenem reveals the mechanism of carbapenem against Mycobacterium tuberculosis. *Cell Res.* **23,** 728–31 (2013).

175. Lecoq, L., Bougault, C., Hugonnet, J.-E., Arthur, M. & Jean-Pierre, S. Structure of Enterococcus faecium L,D-Transpeptidase Acylated by Ertapenem Provides Insight into the Inactivation Mechanism. *ACS Chem. Biol.* **8,** 1140–1146 (2013).

176. Cordillot, M. *et al.* In Vitro Cross-Linking of Mycobacterium tuberculosis Peptidoglycan by L,D-Transpeptidases and Inactivation of These Enzymes by Carbapenems. *Antimicrob. Agents Chemother.* **57,** 5940–5 (2013).

177. Ebina, T., Toh, H. & Kuroda, Y. Loop-length-dependent SVM prediction of domain linkers for high-throughput structural proteomics. *Biopolymers* **92,** 1–8 (2009).

178. Cole, C., Barber, J. D. & Barton, G. J. The Jpred 3 secondary structure prediction server. *Nucleic Acids Res.* **36,** W197–201 (2008).

179. Bielnicki, J. *et al.* B. subtilis ykuD Protein at 2.0 Å Resolution: Insights into the Structure and Function of a Novel, Ubiquitous Family of Bacterial Enzymes. *Proteins Struct. Funct. Bioinforma.* **151,** 144–151 (2006).

180. Djoko, K. Y. *et al.* Conserved Mechanism of Copper Binding and Transfer . A Comparison of the Copper-Resistance Proteins PcoC from Escherichia coli and CopC from Pseudomonas syringae. *Inorg. Chem.* **46,** 4560–4568 (2007).

181. Tan, T., Mijts, B. N., Swaminathan, K., Patel, B. K. C. & Divne, C. Crystal Structure of the Polyextremophilic α -Amylase AmyB from Halothermothrix orenii : Details of a Productive Enzyme – Substrate Complex and an N Domain with a Role in Binding Raw Starch. *J. Mol. Biol.* **378,** 852–870 (2008).

182. Hekmat, O., Leggio, L. Lo, Rosengren, A., Kamarauskaite, J. & Stalbrand, H. Rational Engineering of Mannosyl Binding in the Distal Glycone Subsites of Cellulomonas fimi Endo-β-1 , 4-mannanase: Mannosyl Binding Promoted at Subsite - 2 and Demoted at Subsite - 3. *Biochemistry* **49,** 4884–4896 (2010).

183. Correale, S., Ruggiero, A., Capparelli, R., Pedone, E. & Berisio, R. Structures of free and inhibited forms of the L,D-transpeptidase LdtMt1 from Mycobacterium tuberculosis. *Acta Crystallogr. D. Biol. Crystallogr.* **69,** 1697–706 (2013).

184. Dubée, V. *et al.* Inactivation of Mycobacterium tuberculosis L,D-Transpeptidase Ldt Mt1 by Carbapenems and Cephalosporins. *Antimicrob. Agents Chemother.* **56,** 4189–4195 (2012).

185. Freundlich, J. S. *et al.* Triclosan Derivatives : Towards Potent Inhibitors of Drug- Sensitive and Drug-Resistant Mycobacterium tuberculosis. *ChemMedChem* **4,** 241–248 (2009).

186. Wolucka, B. A., McNeil, M. R., de Hoffmann, E., Chojnacki, T. & Brennan, P. J. Recognition of the Lipid Intermediate for Arabinogalactadkabinomannan Biosynthesis and Its Relation to the Mode of Action of Ethambutol on Mycobacteria. *J. Biol. Chem.* **269,** 23328–23335 (1994).

187. Mikusová, K., Slayden, R. A., Besra, G. S. & Brennan, P. J. Biogenesis of the mycobacterial cell wall and the site of action of ethambutol. *Antimicrob Agents Chemother* **56,** 1797–1809 (2012).

188. Jia, L. *et al.* Interspecies pharmacokinetics and in vitro metabolism of SQ109. *Br. J. Pharmacol.* **147,** 476–485 (2006).

189. Tahlan, K. *et al.* SQ109 targets MmpL3, a membrane transporter of trehalose monomycolate involved in mycolic acid donation to the cell wall core of Mycobacterium tuberculosis. *Antimicrob. Agents Chemother.* **56,** 1797–809 (2012).

190. Kluge, A. F. & Petter, R. C. Acylating drugs : redesigning natural covalent inhibitors. *Curr. Opin. Chem. Biol.* **14,** 421–427

191. Nampoothiri, K. M. *et al.* Molecular cloning , overexpression and biochemical characterization of hypothetical b -lactamases of Mycobacterium tuberculosis H37Rv. *J. Appl. Microbiol.* **105,** 59–67 (2008).